Ocean-Atmosphere Coupling during Monsoon Onset and Intraseasonal Oscillations in the Indian Ocean

Heather L. Roman-Stork

University of South Carolina

June 30, 2020

Motivation

- The southwest monsoon is a dynamically complex system that impacts over a billion people, but current forecasting is inadequate
- 2019 was the first strong monsoon in 25 years
  - Intraseasonal oscillations significantly contribute to monsoon rainfall and modulate the active and break phases of the monsoon
  - Freshwater input from the Bay of Bengal into the southeastern Arabian Sea is a key driver of monsoon onset and strength
- Mesoscale and submesoscale eddies play a major role in general circulation and air-sea interactions in the Bay of Bengal and feedback into monsoon convection

OUTLINE

- The Role of Salinity in Determining Southwest Monsoon Onset and Variability
- Tropical Cyclone and Intraseasonal Oscillation Interactions in the Indian Ocean
- Intraseasonal Oscillations in the Indian Ocean
- Eddy Variability and Connections to Atmospheric Convection in the Bay of Bengal

OVERVIEW

- Northern basin – no connection to any open oceans
- Pacific Ocean and the ITF – warm, fresh water
- Seasonal reversal of winds and currents
- Southwest monsoon: June to September
- Northeast monsoon: November to February
- Purple star = Kerala

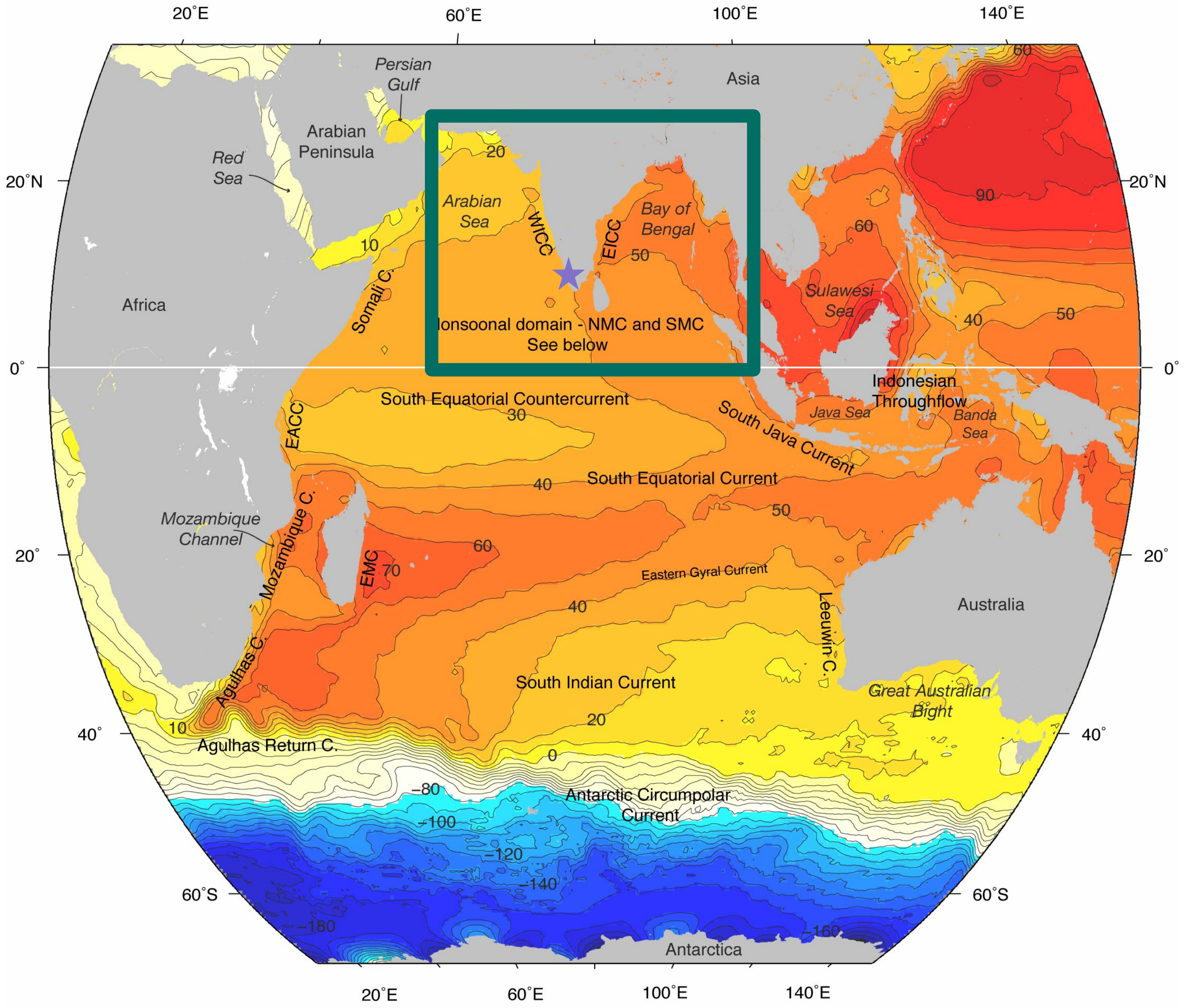

Surface circulations and dynamic ocean topography (cm) in the Indian Ocean (Talley, 2011)

MONSOON ONSET

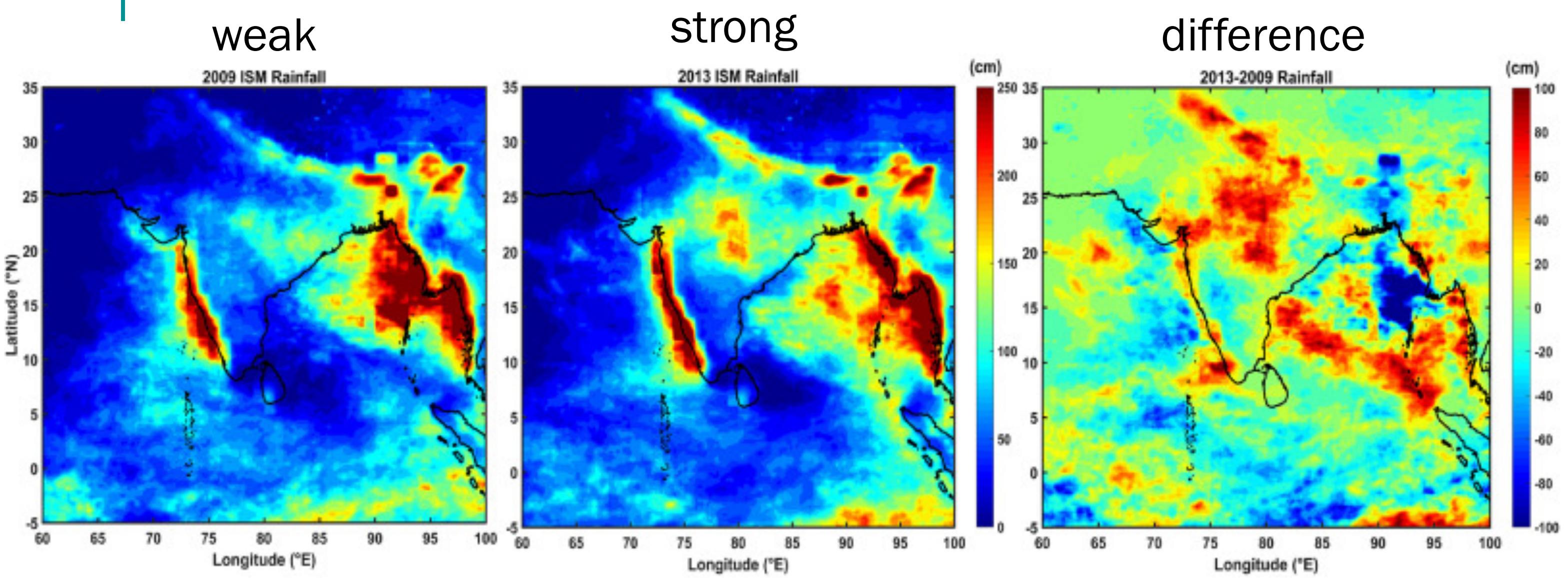

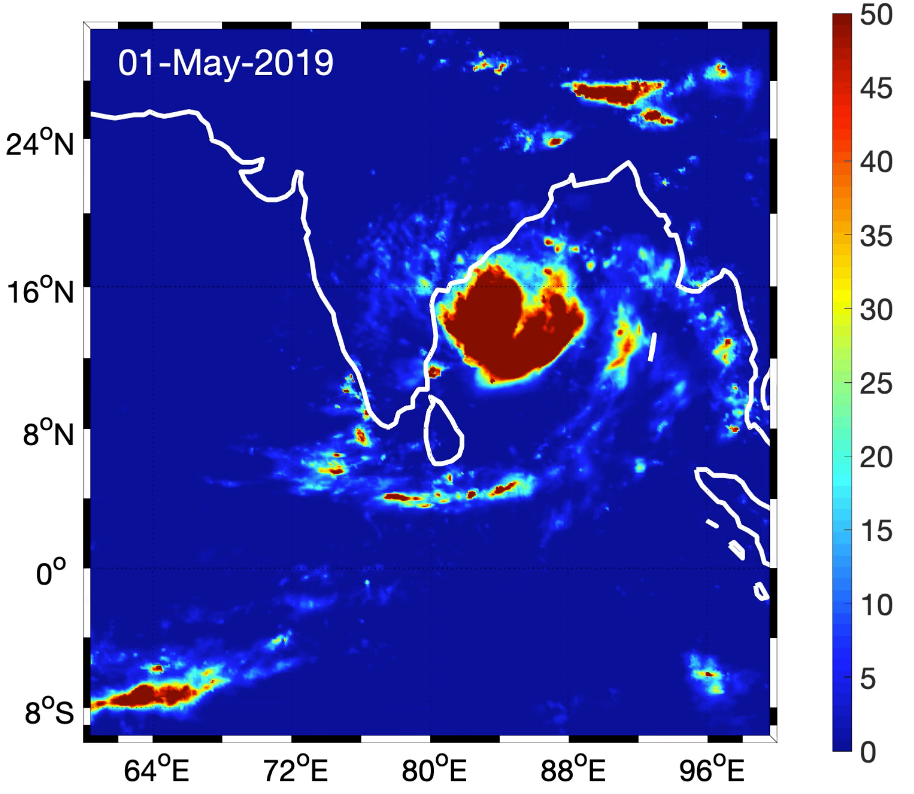

- Seasonal southwest monsoon rainfall distribution
- More rainfall over central India, the Bay of Bengal (BoB) during a stronger monsoon

- 2019 Monsoon onset ~June 9
  - First strong monsoon since 1994
  - Can see onset over Kerala
  - MOV propagates North along coast

TRMM ISM season rainfall (cm) for the years 2009, 2013 and the seasonal rainfall difference (2013–2009). From Gulakaram et al,. (2018).

GPM Daily Precipitation (mm/day)

SOUTHWEST MONSOON RAINFALL

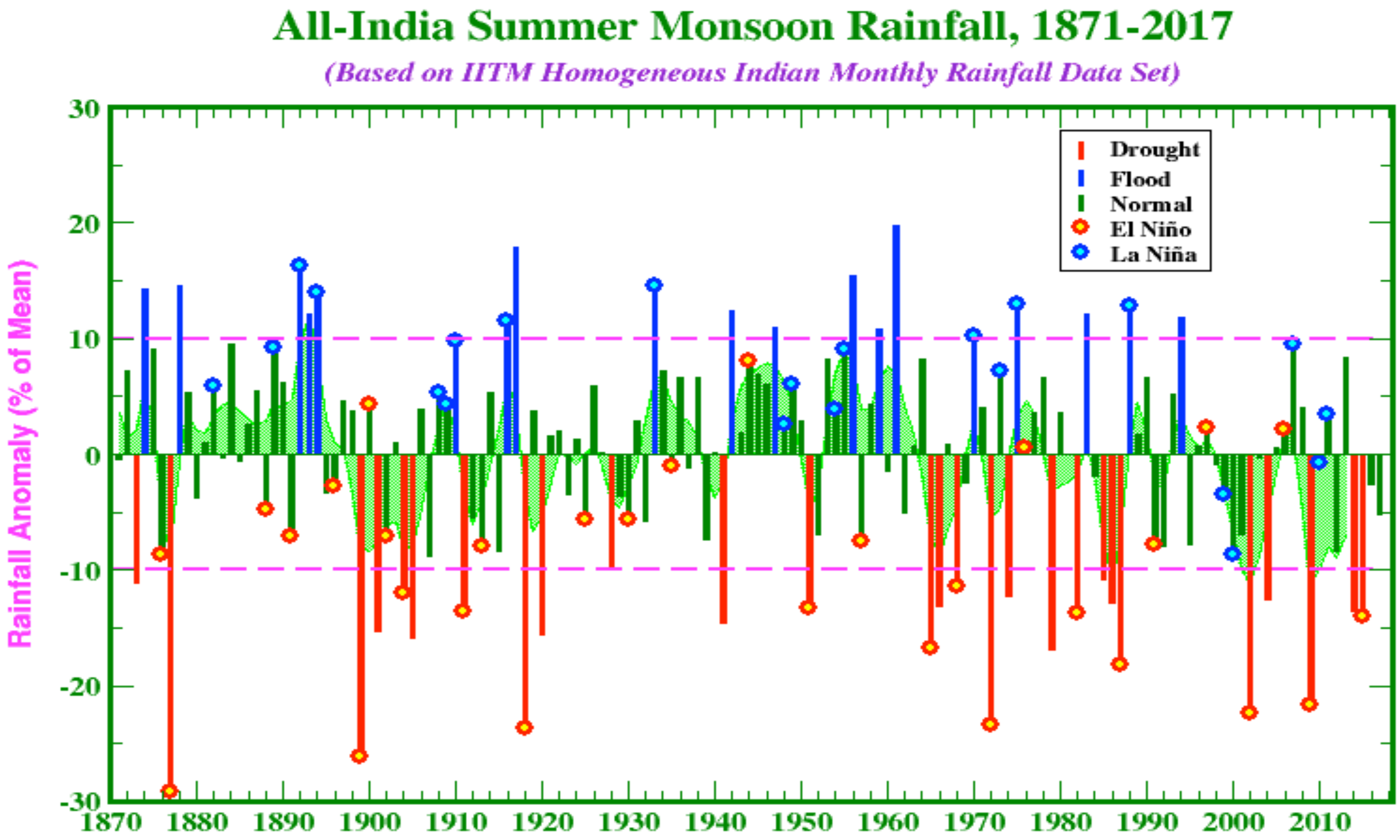

- Strong monsoons: >10% **above** the long-term mean rainfall
- Weak monsoons: >10% **below** the long-term mean rainfall
- Last strong monsoon was 1994 until 2019 strong monsoon
- Indian Ocean Dipole (IOD) and El Niño-Southern Oscillation (ENSO) help modulate monsoon strength

SALINITY EXCHANGE

- Seasonal exchange between Arabian Sea and BoB around the tip of India and Sri Lanka
- Fresher water from the BoB accumulates following southwest monsoon season and is transported to Arabian Sea between October and January by the East India Coastal Current (EICC)

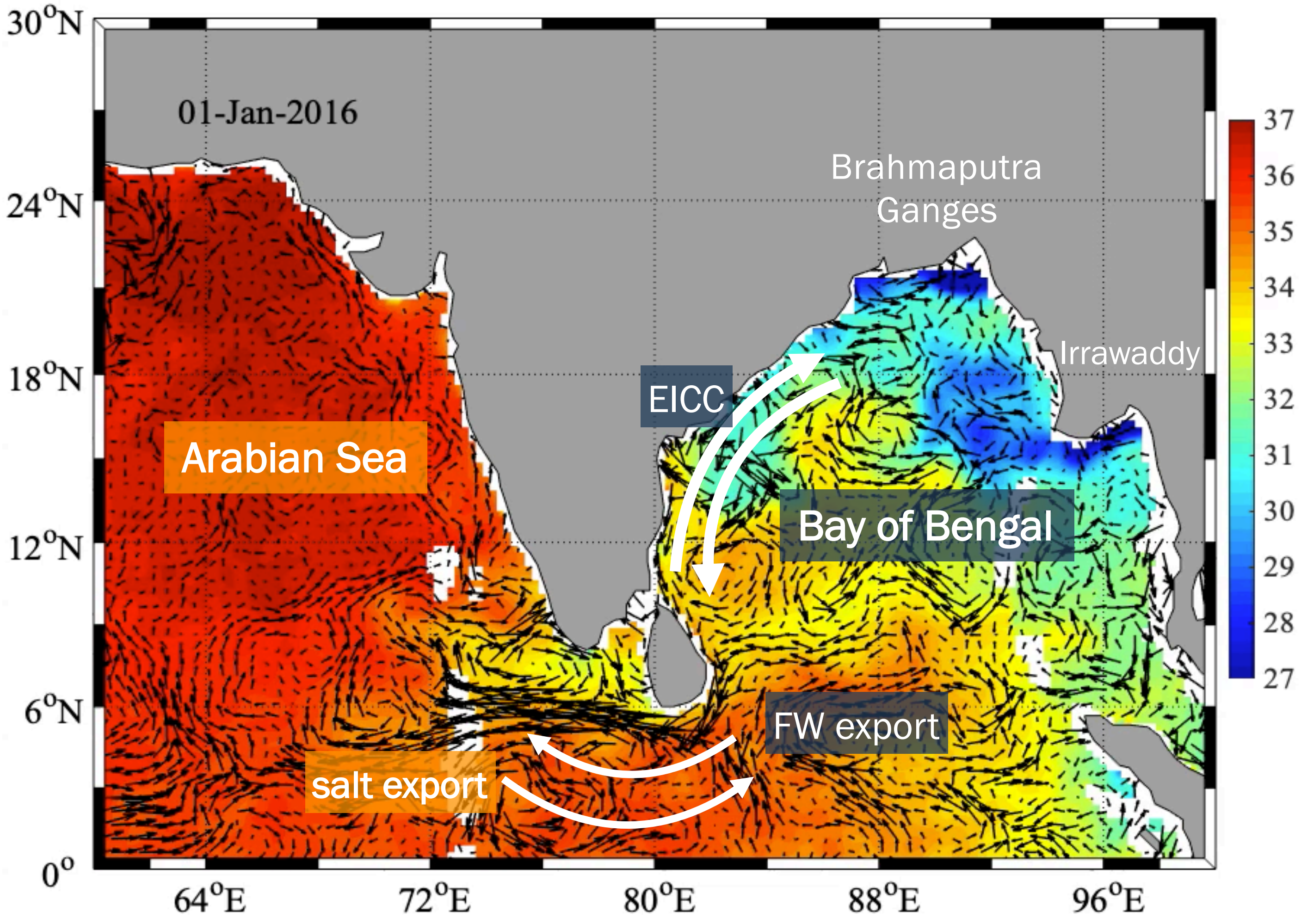

SMAP salinity (shaded; psu) with altimetry derived surface currents in the northern Indian Ocean from 2016 to 2018.

The Role of Salinity in Determining Southwest Monsoon Onset and Variability

OCEANIC CONDITIONS FOR MONSOON ONSET

5. ITCZ moves over the SST high by end of May, increasing both SST and large-scale moisture convergence. Genesis of the monsoon onset vortex!

4. High April SSTs trigger pre-monsoon rainfall (insufficient moisture for full onset)

1. Southwest monsoon collapses in October and the northeast monsoon strengthens, triggering EICC and westward flow

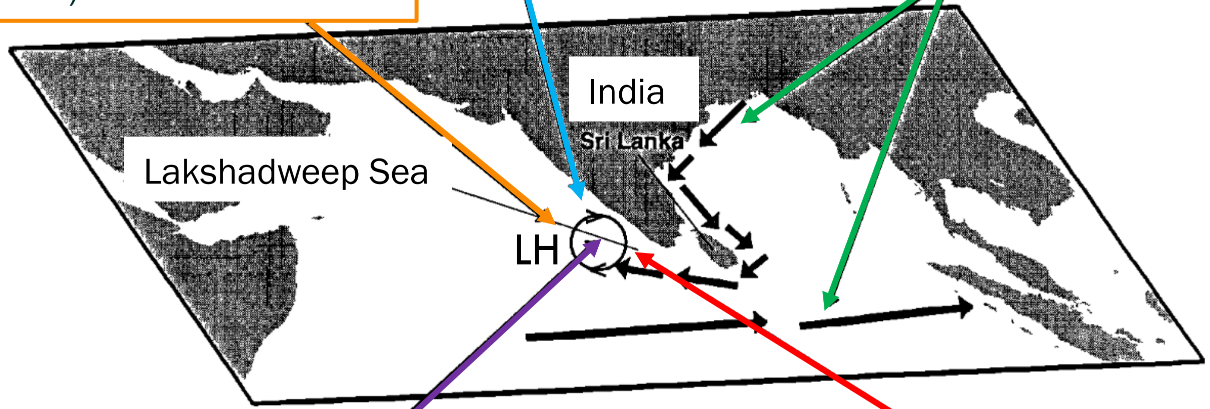

3. Stable stratification & downwelling provide conditions favorable to surface warming, leading to higher SSTs by March

2. By January, a region of high sea level and low SSS forms in Lakshadweep Sea

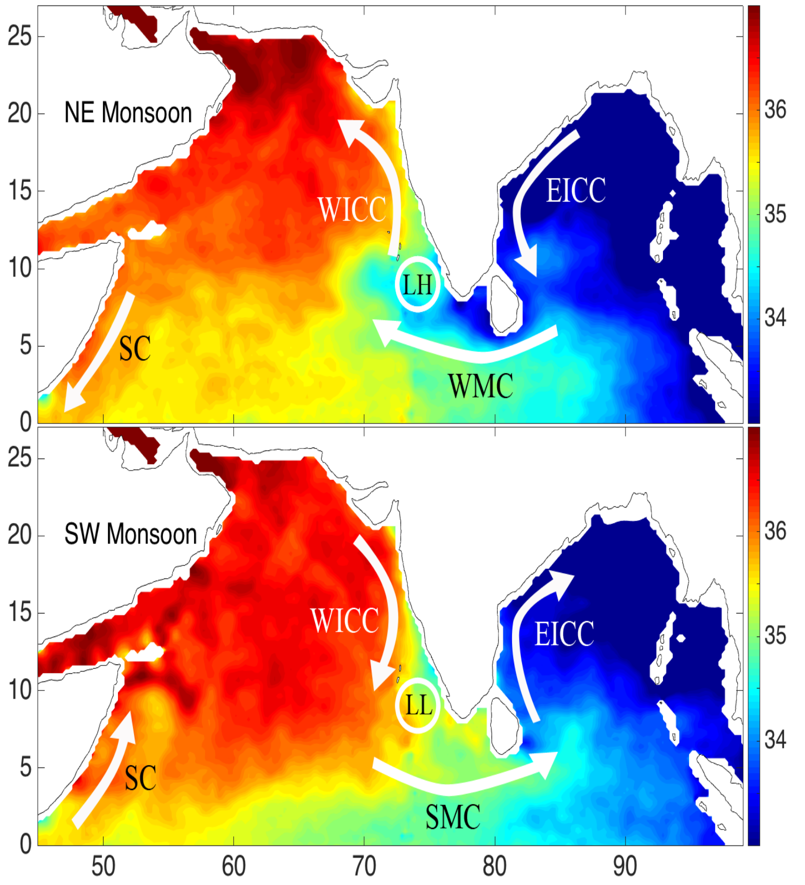

SMAP SSS during the NE and SW Monsoons of 2016 (figure courtesy of Corinne Trott)

Left: adapted from Shenoi et al. (1999)

SATELLITE SALINITY

Soil Moisture & Ocean Salinity (SMOS) Mission by European Space Agency
L-band radiometer

Aquarius/SAC-D Mission by NASA & CONAE
L-band radiometer + radar

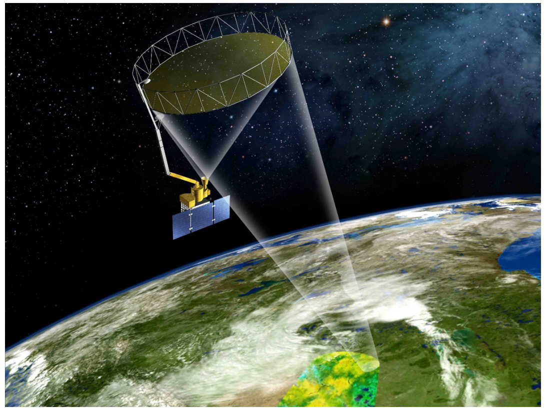

NASA's Soil Moisture Active-Passive (SMAP), January 2015-present
L-band radiometer + radar
(radar stopped functioning July 2015)

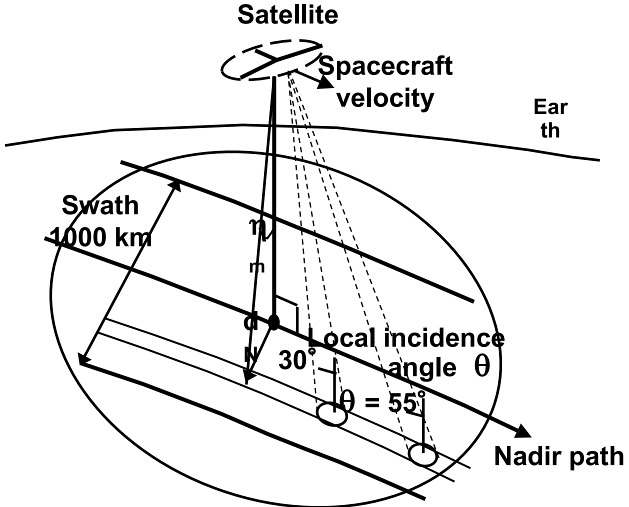

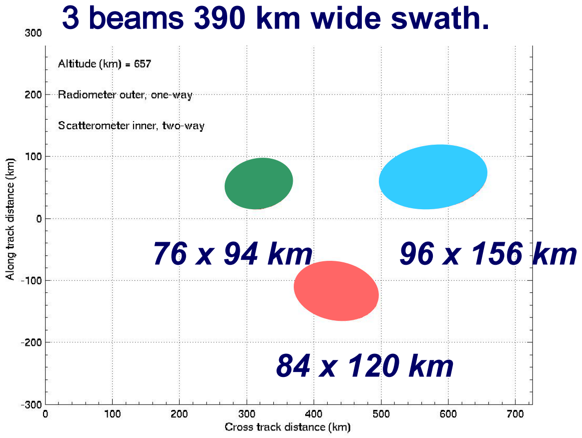

Full 360° scan views the Earth. 1000 km wide swath. 3-dB (half power) footprint size: 40 km. Time for sampling 1 footprint: 17 msec.

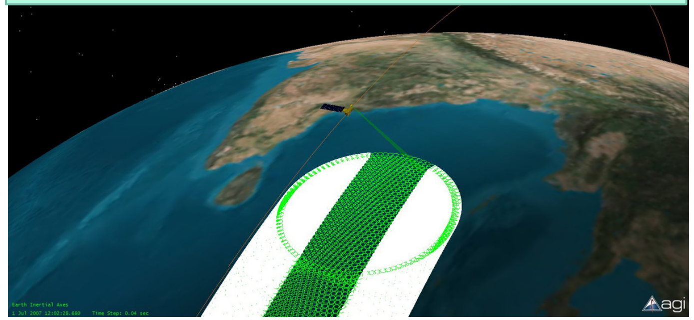

SEAS SALINITY

- Composite SMAP SSS in December (shaded; psu)
- Taylor diagram of different SSS products in the SEAS
- Comparative time series of SSS in the SEAS with shaded standard deviation

A) Monthly averaged SMAP sea surface salinity (SSS) for December 2016-2018 (shaded; psu) and the black box indicates the SEAS region (6°-13°N, 65°-75°E); B) Taylor diagram comparing multiple SSS products for the SEAS region; and C) Comparison of time series of various products of SSS with one standard deviation (shaded) for the SEAS region from 1980 to 2016.

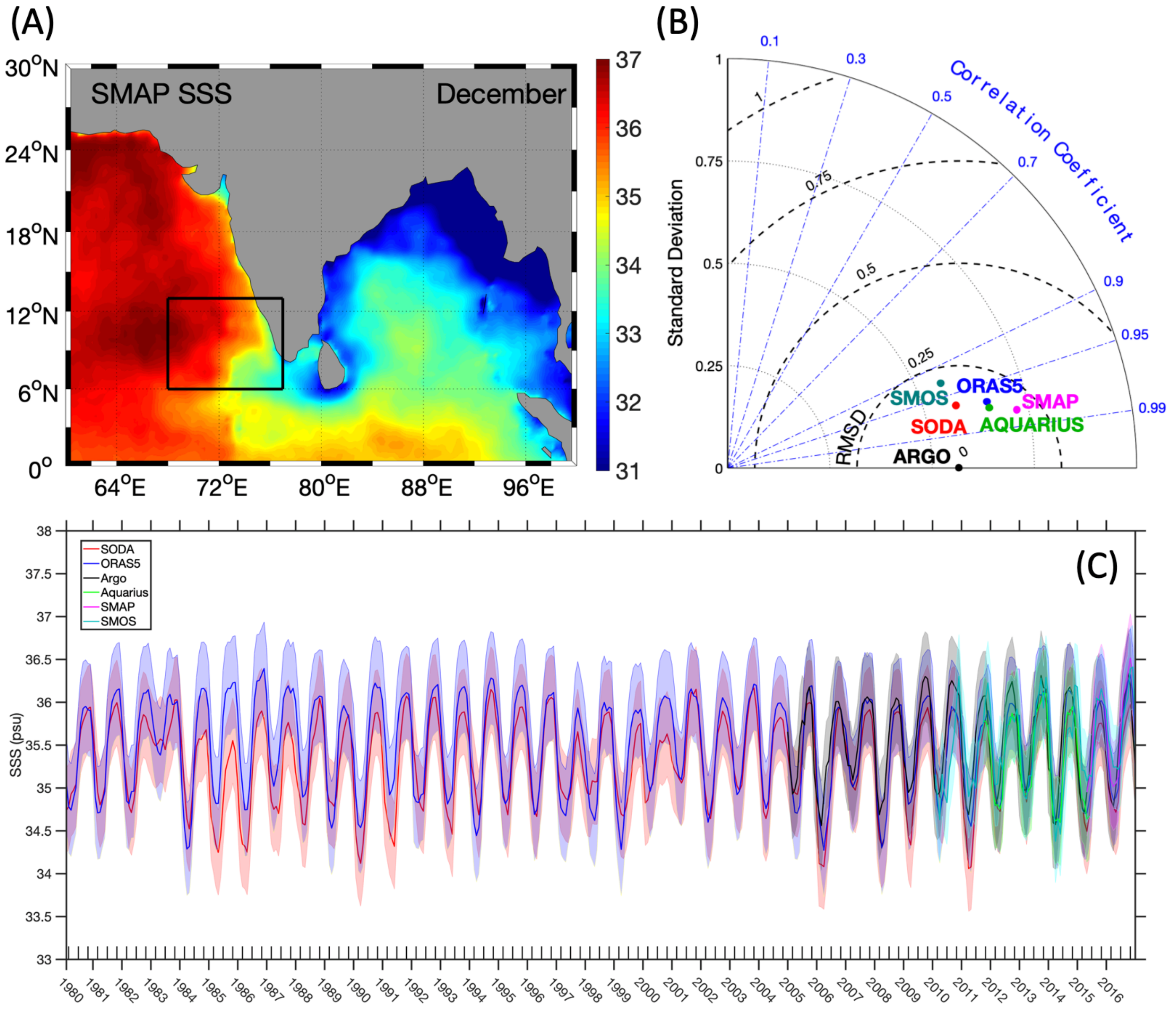

Roman-Stork et al., (2020)

BARRIER LAYER DEVELOPMENT

- ORAS5 has higher salinity values at depth, higher SSTs
- Lower salinity (<35 psu) values reach to 40-60 m
- Lower salinity values and deeper BLT for weak monsoon regime
- White line = BLT
- Magenta line = April of monsoon year

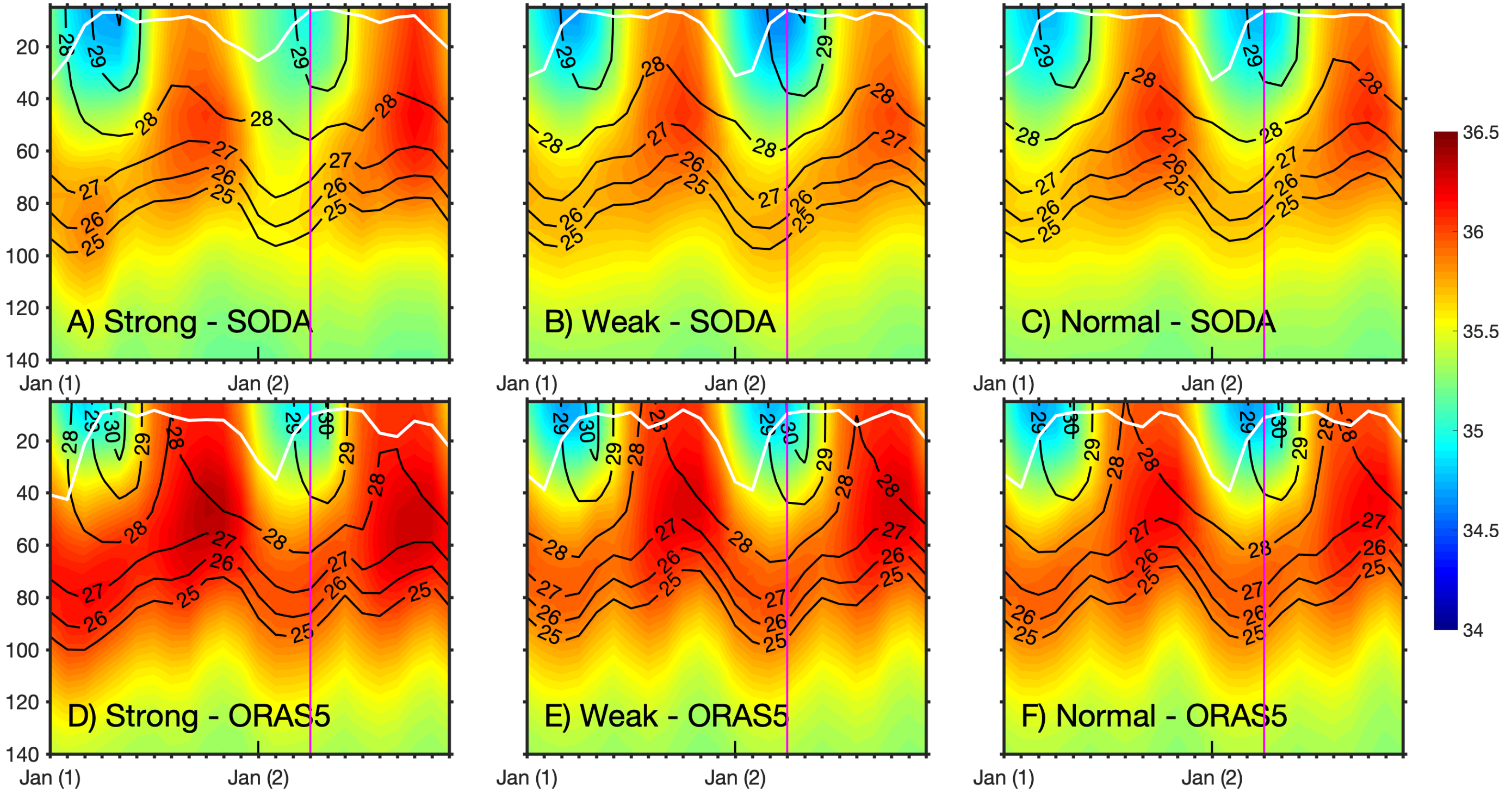

Composite time-depth plots of (A-C) SODA and (D-F) ORAS5 products of salinity (shaded; psu) and temperature (contours; °C) with overlaid barrier layer thickness (BLT in m, white line) calculated for each product in the SEAS region (6°-13ºN, 65°-75ºE) leading to and during a strong (1st column), weak (2nd column), and normal (3rd column) monsoon. A pink vertical line is drawn for April month of the given monsoon season. From Roman-Stork et al., (2020).

SALT BUDGET

- Composite time series of salt budget terms in psu/month:
  - A) surface freshwater flux (SFWF)
  - B) zonal advection
  - C) meridional advection
  - D) entrainment
  - E) the sum of terms A-D (solid lines) and the salinity tendency (dS/dt; dashed lines)
  - For the SEAS region (6° -13ºN, 65° -75ºE) comparing a composite strong (blue), weak (red), and **normal** (black) southwest monsoon season.
- Advective processes dominate salinity in the SEAS → EICC and NEC transport

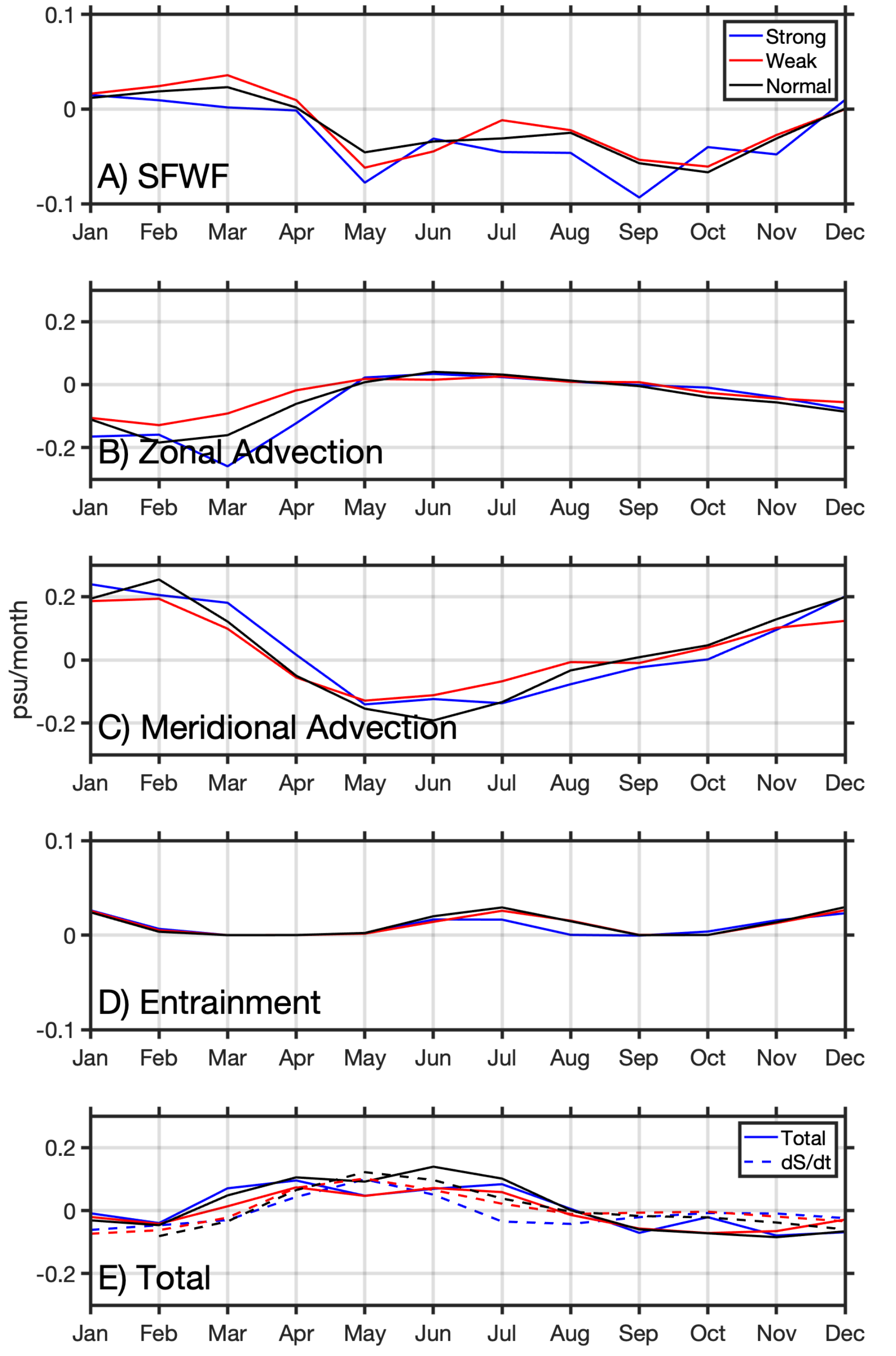

Composite time series of salt budget terms in psu/month a) surface freshwater flux (SFWF), b) zonal advection, c) meridional advection, d) entrainment, and e) the sum of terms a-d (solid lines) and the salinity tendency (dS/dt; dashed lines) for the SEAS region (6°-13ºN, 65°-75ºE) comparing a composite strong (blue), weak (red), and normal (black) southwest monsoon season. From Roman-Stork et al., (2020).

FRESHWATER FLUX

- Weak and normal regimes have strong EICC flow into the Bay of Bengal
- The strong regime has stronger NEC transport into the SEAS through Apr
- Zonal freshwater flux continued into the SEAS through Apr for the strong regime

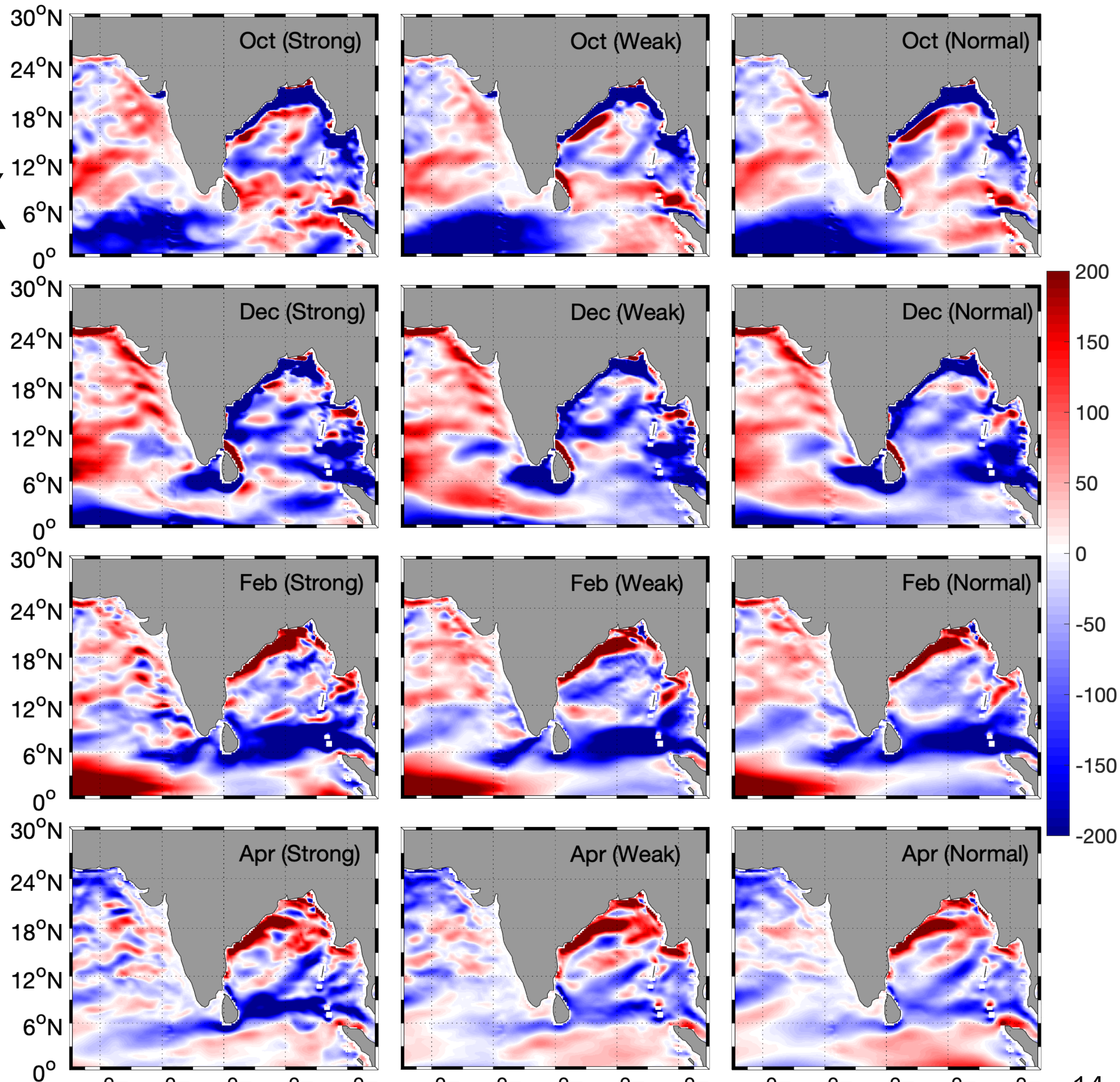

*Bimonthly distributions of **zonal surface advective freshwater flux** (m^2/s) in the northern Indian Ocean for October (1st row), December (2nd row), February (3rd row) and April (4th row) leading to the ensuing strong (left), weak (middle), and normal (right) southwest monsoon season. From Roman-Stork et al., (2020)*

MIXED LAYER PARAMETERS

- Shallower barrier layer before strong monsoon
- Higher (positive) OHC before/after a weak monsoon; higher OHC during a strong monsoon
- Moisture flux much higher (positive) during a strong monsoon, lower (negative) before onset

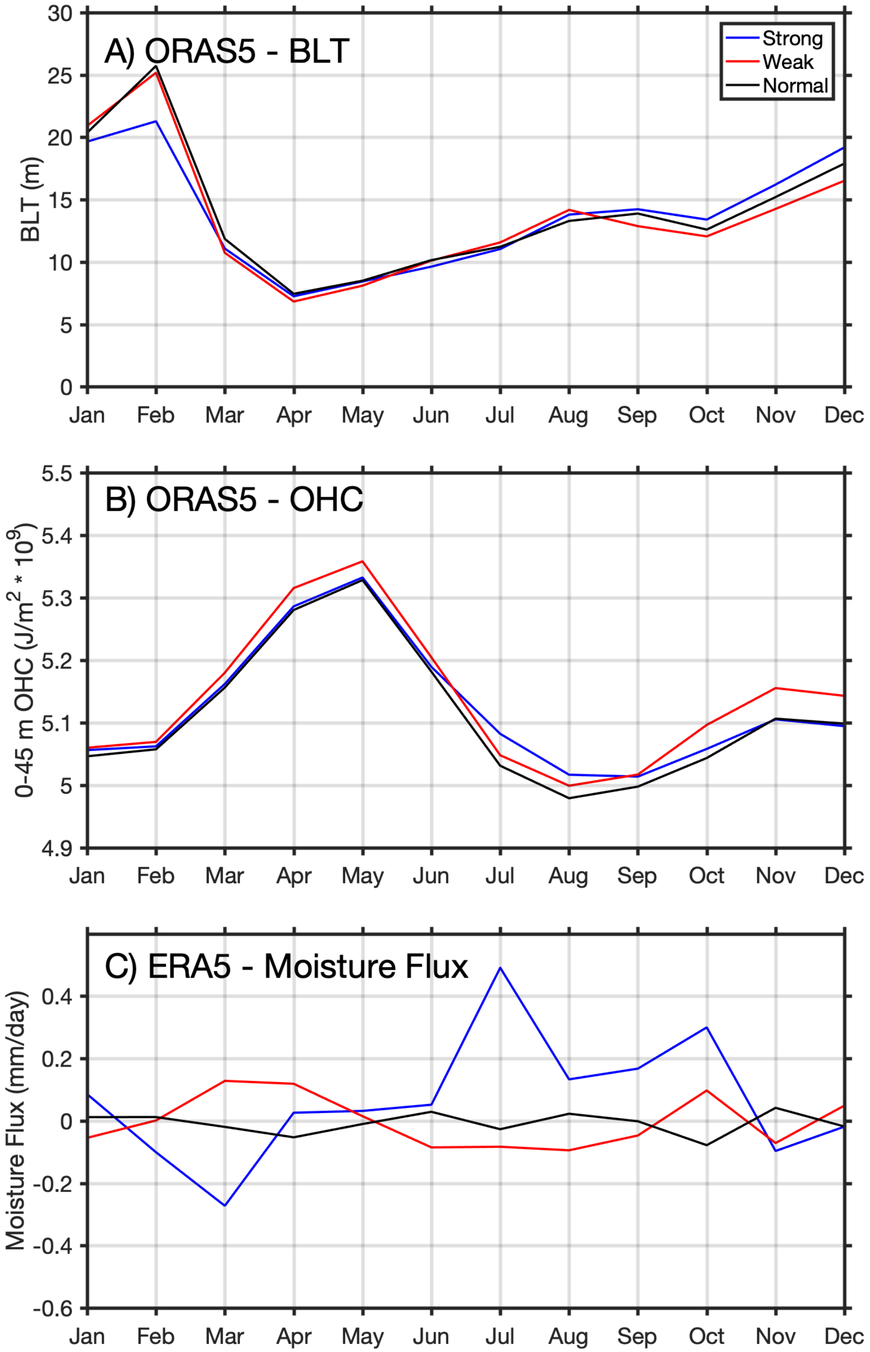

Composite time series of a) ORAS5 barrier layer thickness (BLT; m), b) ORAS5 upper ocean (0-45 m) heat content (10^8 J/m^2), and c) ERA5 instantaneous moisture flux (mm/day) for the SEAS region (6°-13ºN, 65°-75ºE) comparing a composite strong (blue), weak (red), and **normal** (black) southwest monsoon season. From Roman-Stork et al., (2020).*

TRENDS

- Moisture flux, BLTA decrease substantially after 1994
- OHC increasing since 1995 (long-term trend, red line)
- Strong 7, 15-year trends → upward turn likely

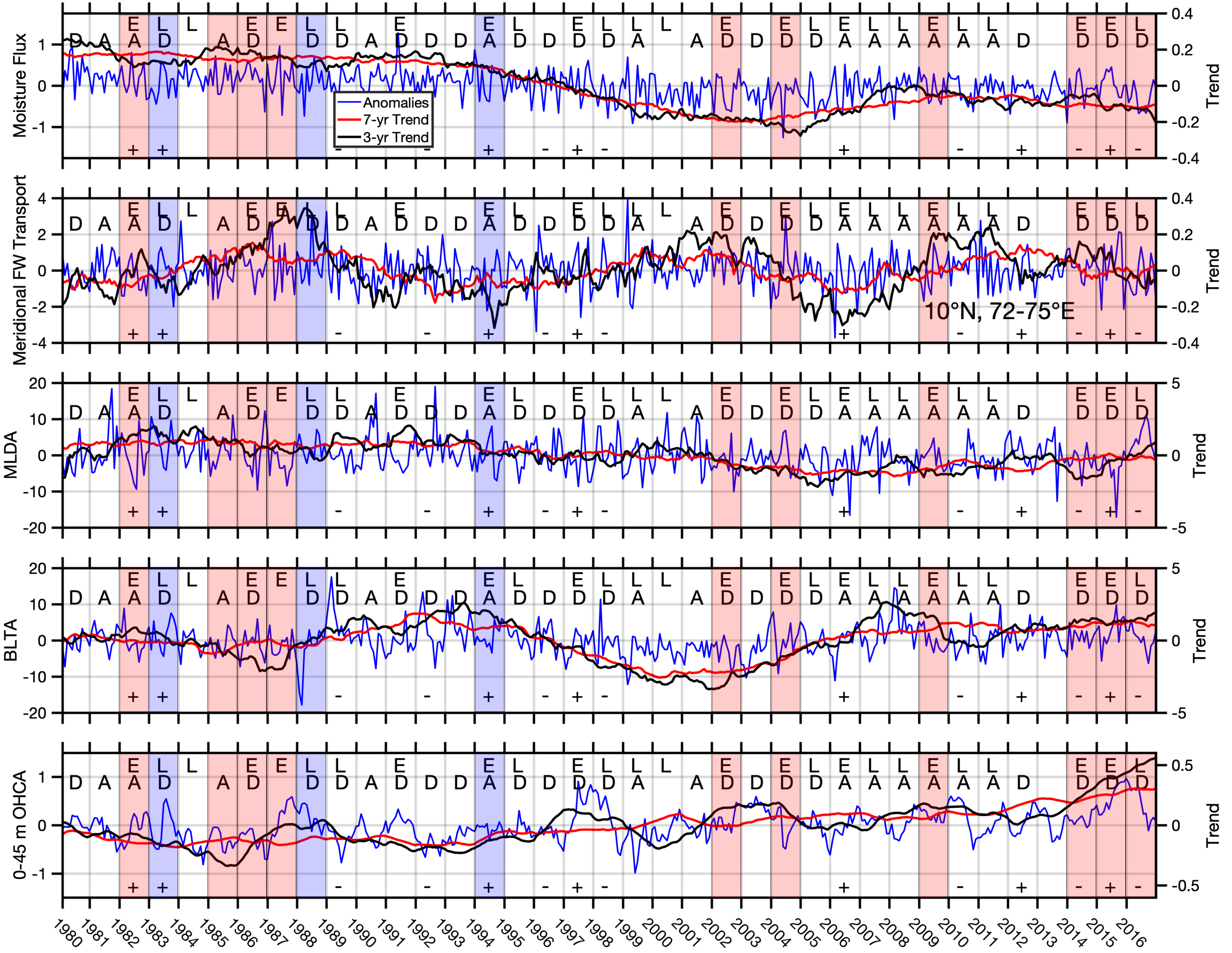

*Time series of ERA5 instantaneous moisture flux anomalies (1st row; blue; mm/day), ORAS5 0-45 m layer meridional freshwater transport anomalies (normalized with its Standard Deviation) at 10°N, 72-75°E (2nd row; blue; * 10^8 kg/s), ORAS5 MLD anomalies (3rd row; m), ORAS5 BLT anomalies (4th row; blue; m), and ORAS5 0-45 m layer OHC anomalies (5th row; blue; J/m^2 *10^8). Red (black) curves indicate a 7-year (3-year) moving mean, whereas red (blue) shading indicates a drought (flood) monsoon year. Occurrences of El Niño (La Niña) are indicated by the letter E (L), MOK is indicated as being delayed (D) or advanced (A), and the occurrences of positive (+) phase and negative phase (-) of an IOD year is also marked. From Roman-Stork et al., (2020).*

Tropical Cyclone and Intraseasonal Oscillation Interactions in the Indian Ocean

AMPHAN (2020)

- Cyclone Amphan (2020): May 16-May 20 in the Bay of Bengal
- Timed with the arrival of the 1st downwelling Kelvin wave

- A) GPM precipitation (mm/day)
- B) CMEMS blended SLA (cm)
- C) OI SST (°C)
- D) SMAP SSS (psu)

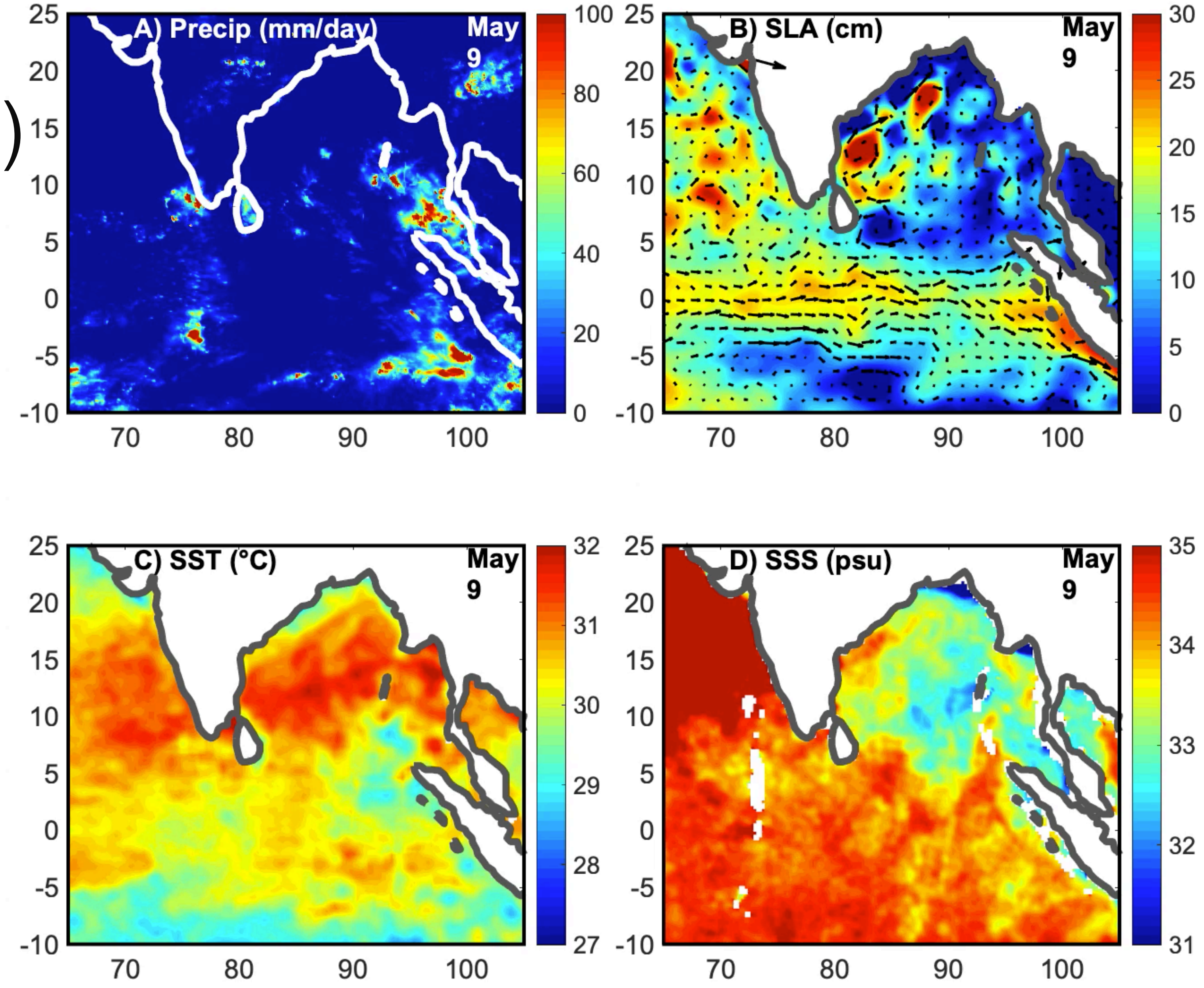

OCEAN COLOR AND TRACK

- Cyclone Amphan (2020) track in the Bay of Bengal
- Formed in southern Bay of Bengal and moved north, making landfall in northern India/Bangladesh
- Upwelling following cyclone passage allows for blooms in the usually anoxic central Bay
- NOAA Coastwatch NRT multi-sensor, gap filled ocean color product allows for cloud-free view of blooms

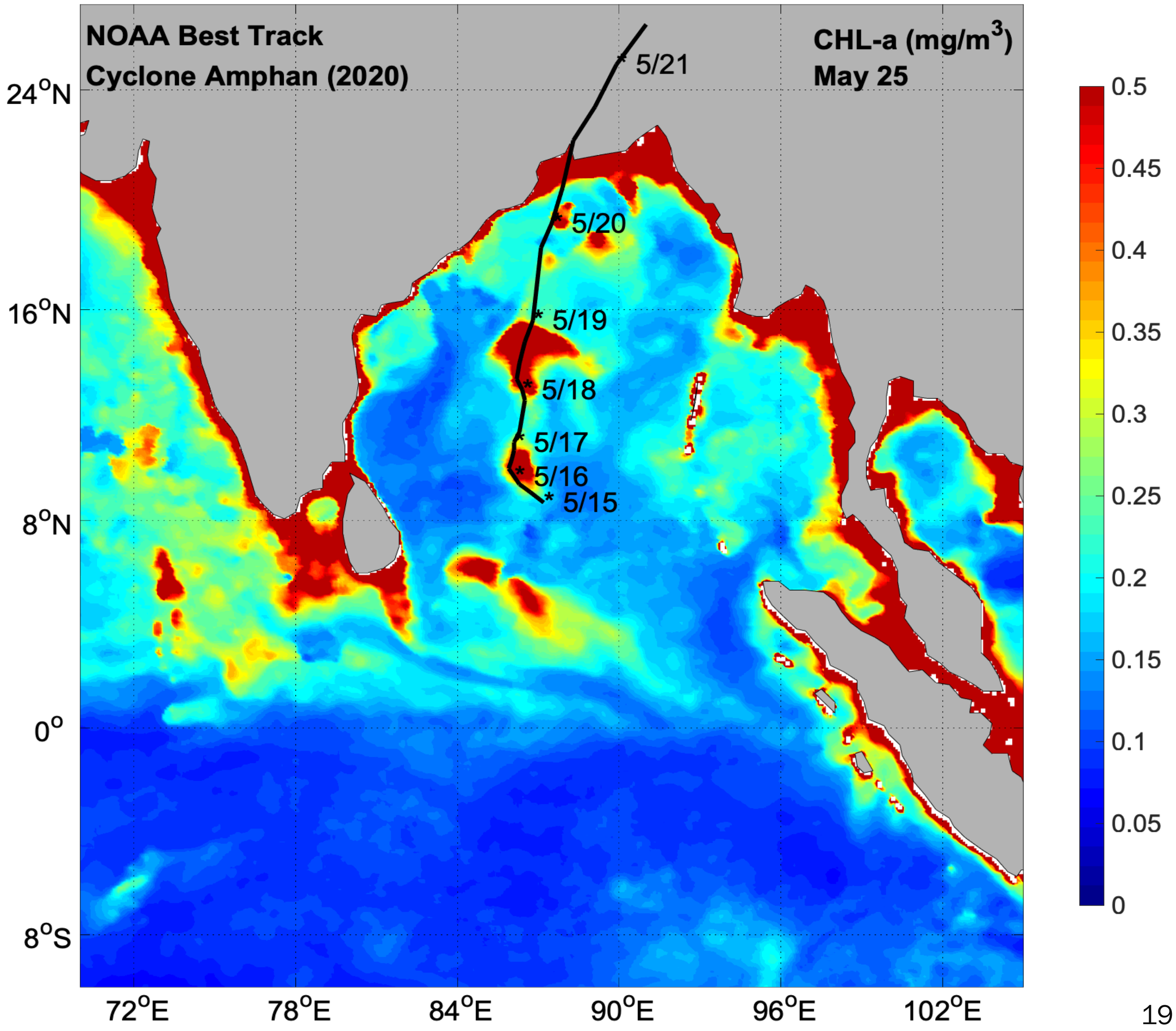

MADDEN-JULIAN OSCILLATIONS (30-90-DAY)

- Commonly defined as 30-90 days, consistent with spectral peaks in precipitation and low-level winds
- Wavelength of 10,000 km
- Reduced cloud-cover vs. enhanced convection
- Equatorially trapped
- Travels eastward and northward (BSISO) over the Bay of Bengal during the southwest monsoon
- Strong air-sea coupling
- Propagates at a rate of 3-5 ms^{-1} and gradually weakens when it reaches the central Pacific

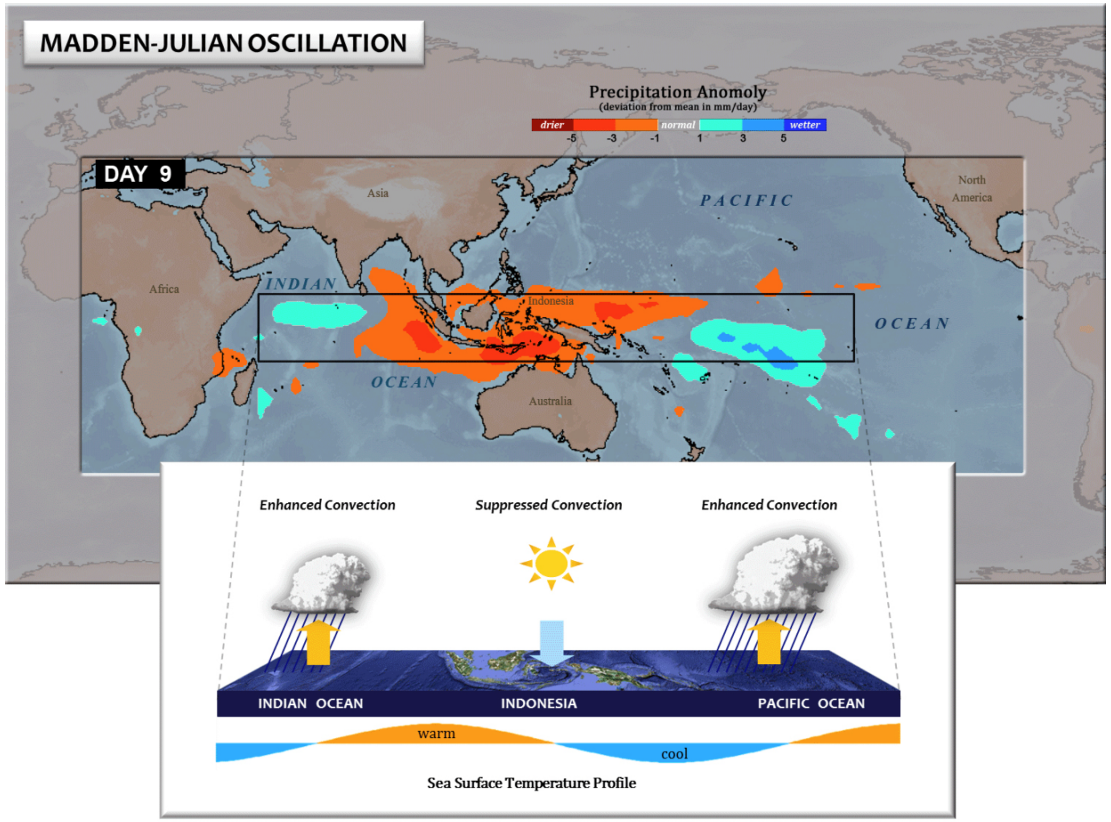

This illustration shows a moment in the evolution of the Madden-Julian Oscillation, a complex process involving sea surface temperatures and their influence on atmospheric processes. (©UCAR. Illustration by Lex Ivey, based on data from Adrian Matthews.)

MJO PROPAGATION

30-90-day filtered

Precip

SLA

SST

SSS

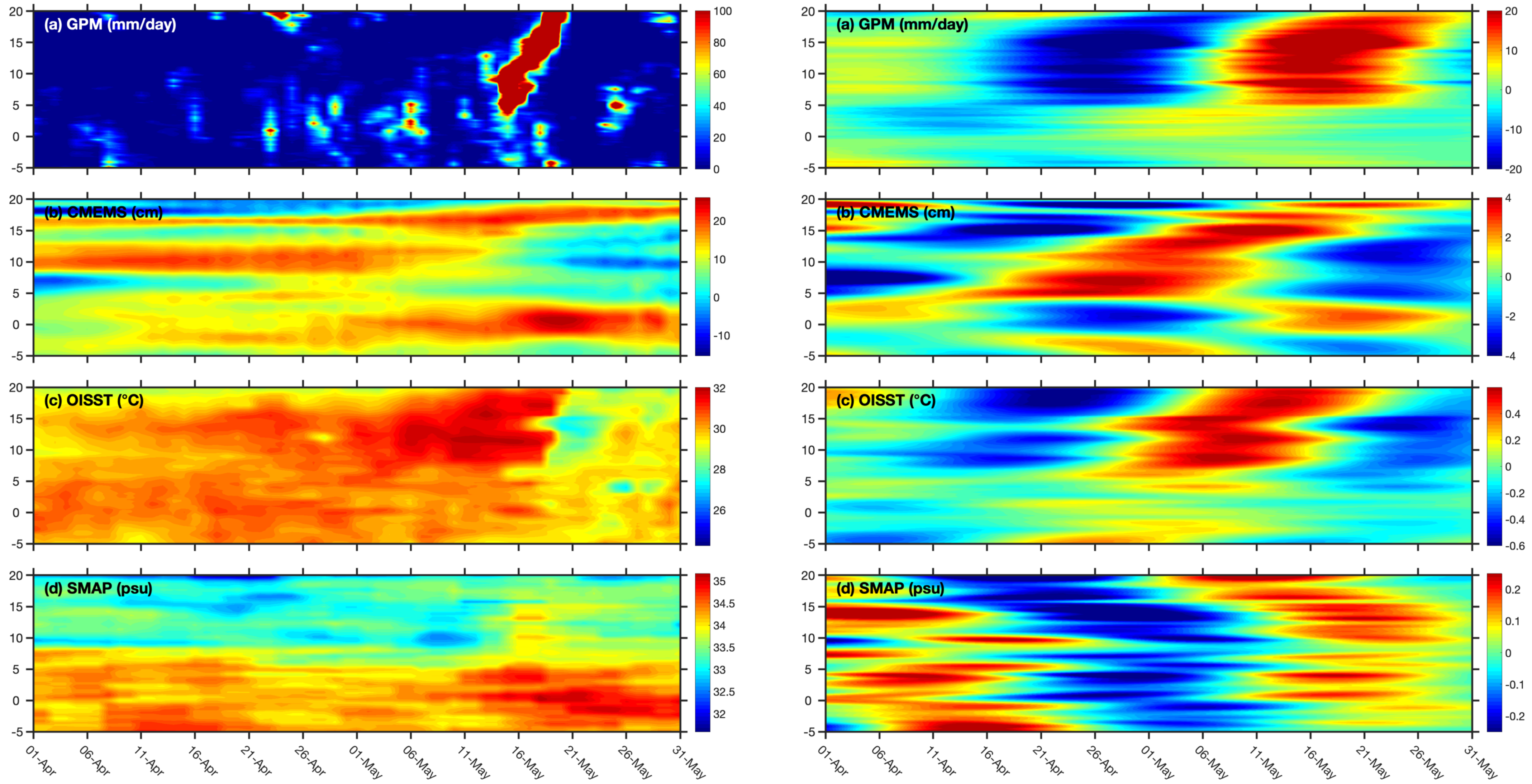

MJO PROPAGATION AND MONSOON ONSET

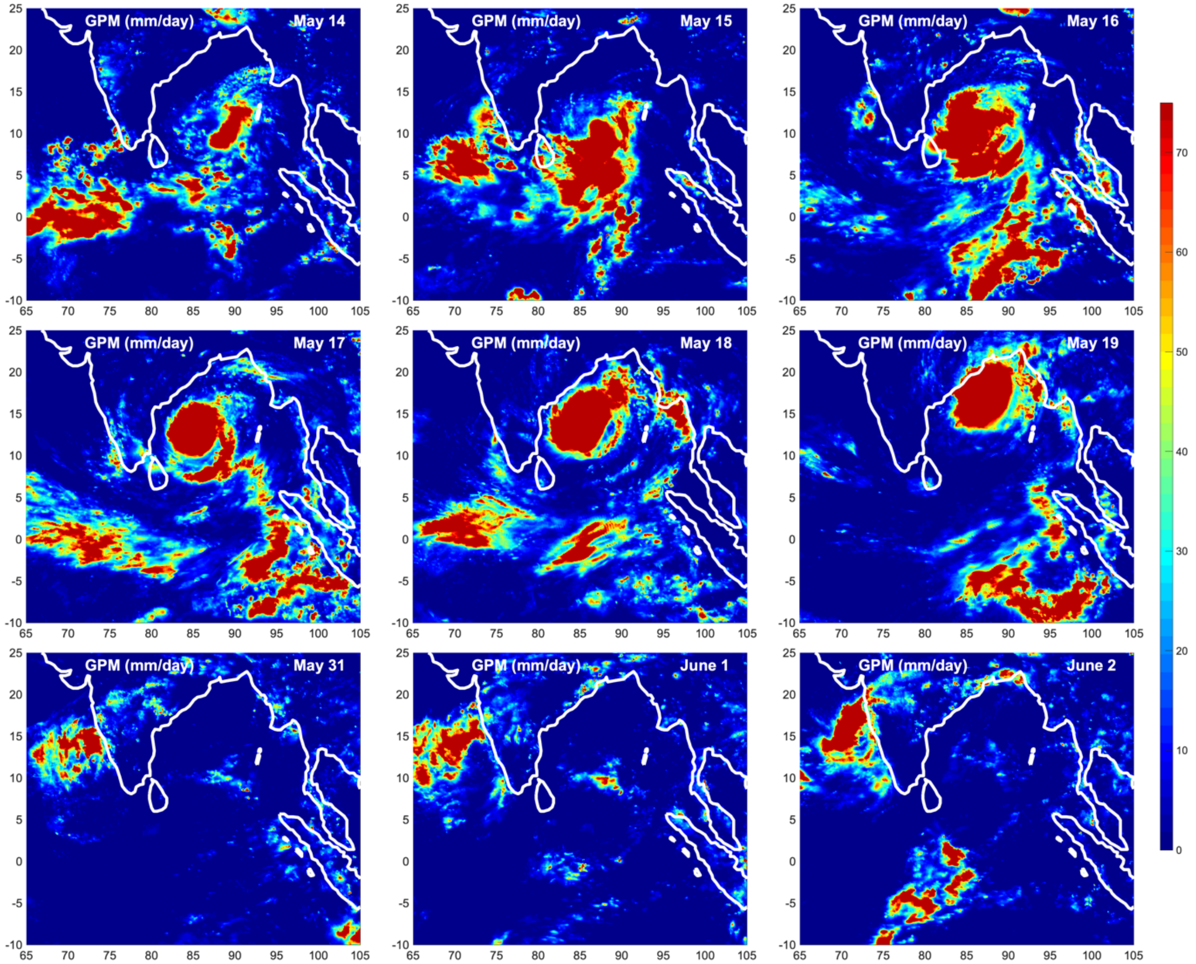

- Northward propagation of MJO helped trigger Amphan in the Bay of Bengal
- MJO propagation also allowed for monsoon preconditioning in the Arabian Sea and led to the timing of monsoon onset on June 1

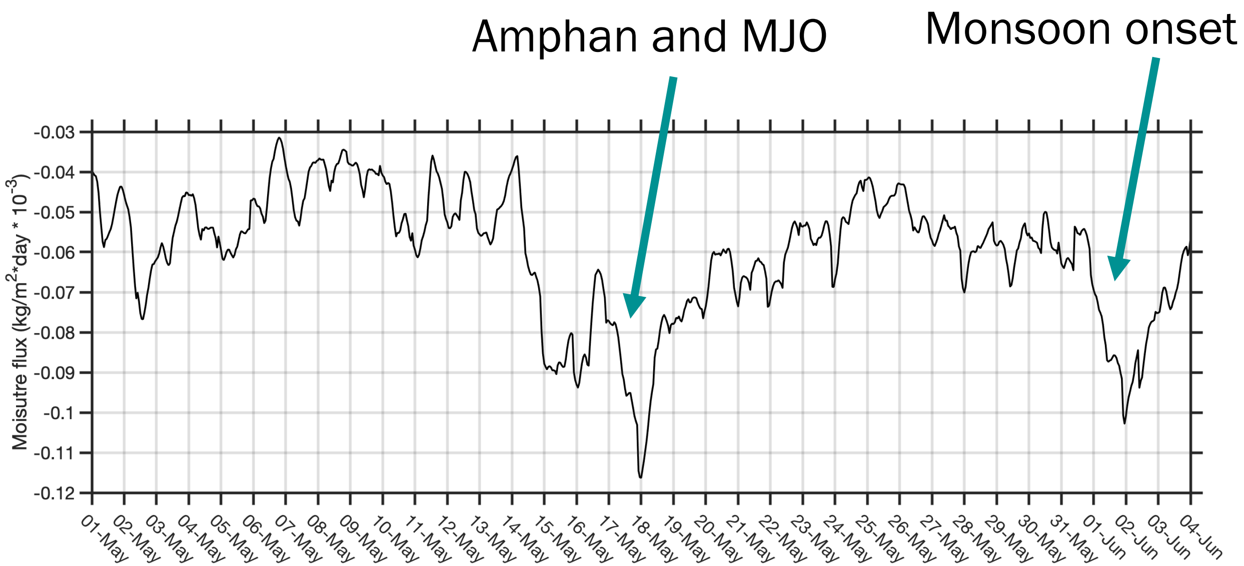

Intraseasonal Oscillations in the Indian Ocean

INTRASEASONAL OSCILLATIONS (ISOs)

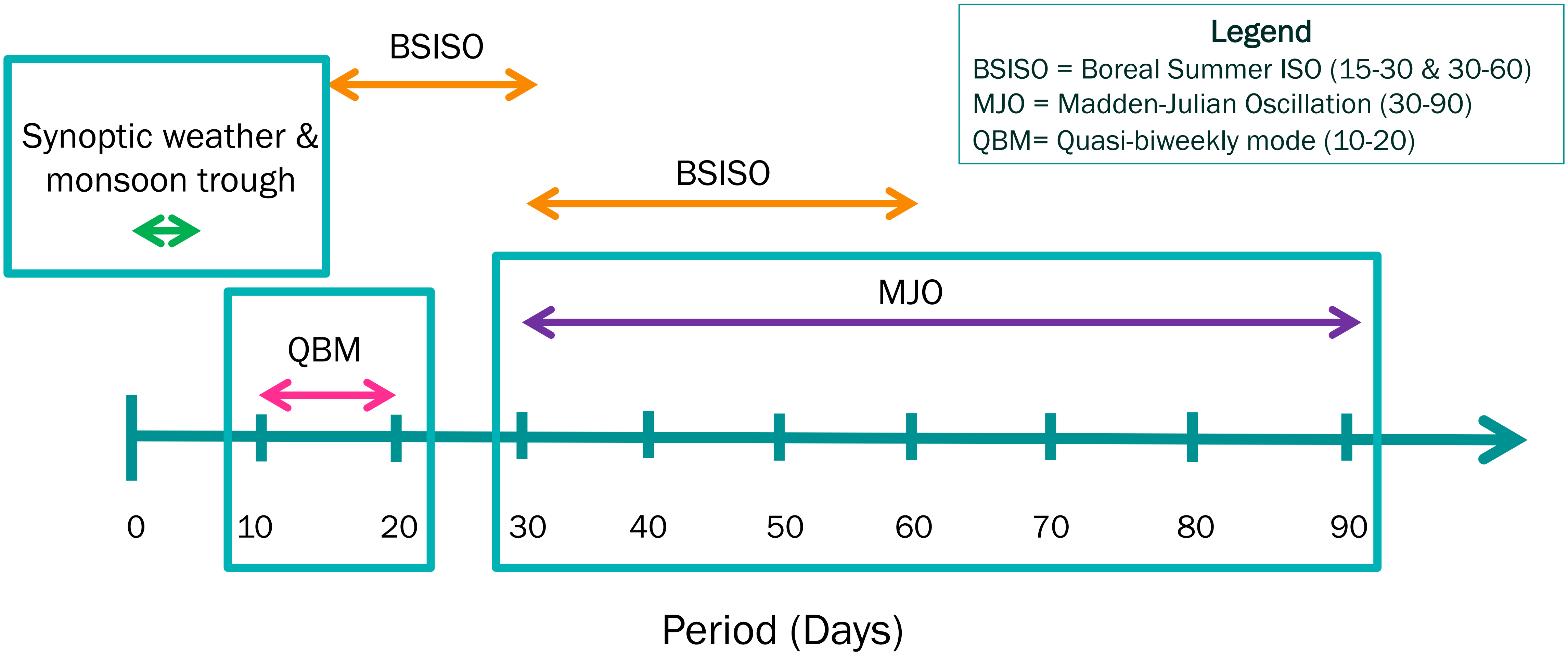

MADDEN-JULIAN OSCILLATIONS (30-90-DAY)

- Commonly defined as 30-90 days, consistent with spectral peaks in precipitation and low-level winds
- Wavelength of 10,000 km
- Reduced cloud-cover vs. enhanced convection
- Equatorially trapped
- Travels eastward and northward (BSISO) over the Bay of Bengal during the southwest monsoon
- Strong air-sea coupling
- Propagates at a rate of 3-5 ms^{-1} and gradually weakens when it reaches the central Pacific

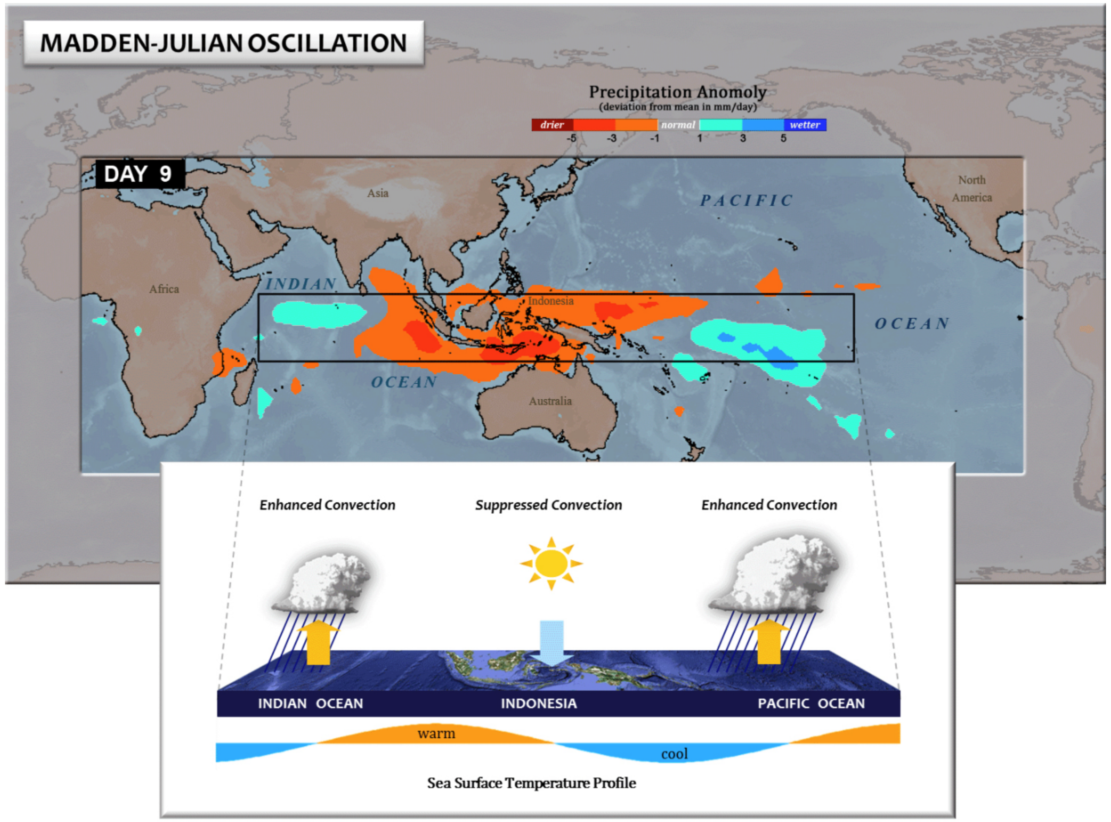

This illustration shows a moment in the evolution of the Madden-Julian Oscillation, a complex process involving sea surface temperatures and their influence on atmospheric processes. (©UCAR. Illustration by Lex Ivey, based on data from Adrian Matthews.)

30-90-DAY ISO

- Comparison of all 5 satellite SSS products from 2010-2017
- SMOS has the strongest MJO signal
- CAP algorithm increases Aquarius magnitude by 50%
- CAP algorithm significantly improves SMAP SSS signal

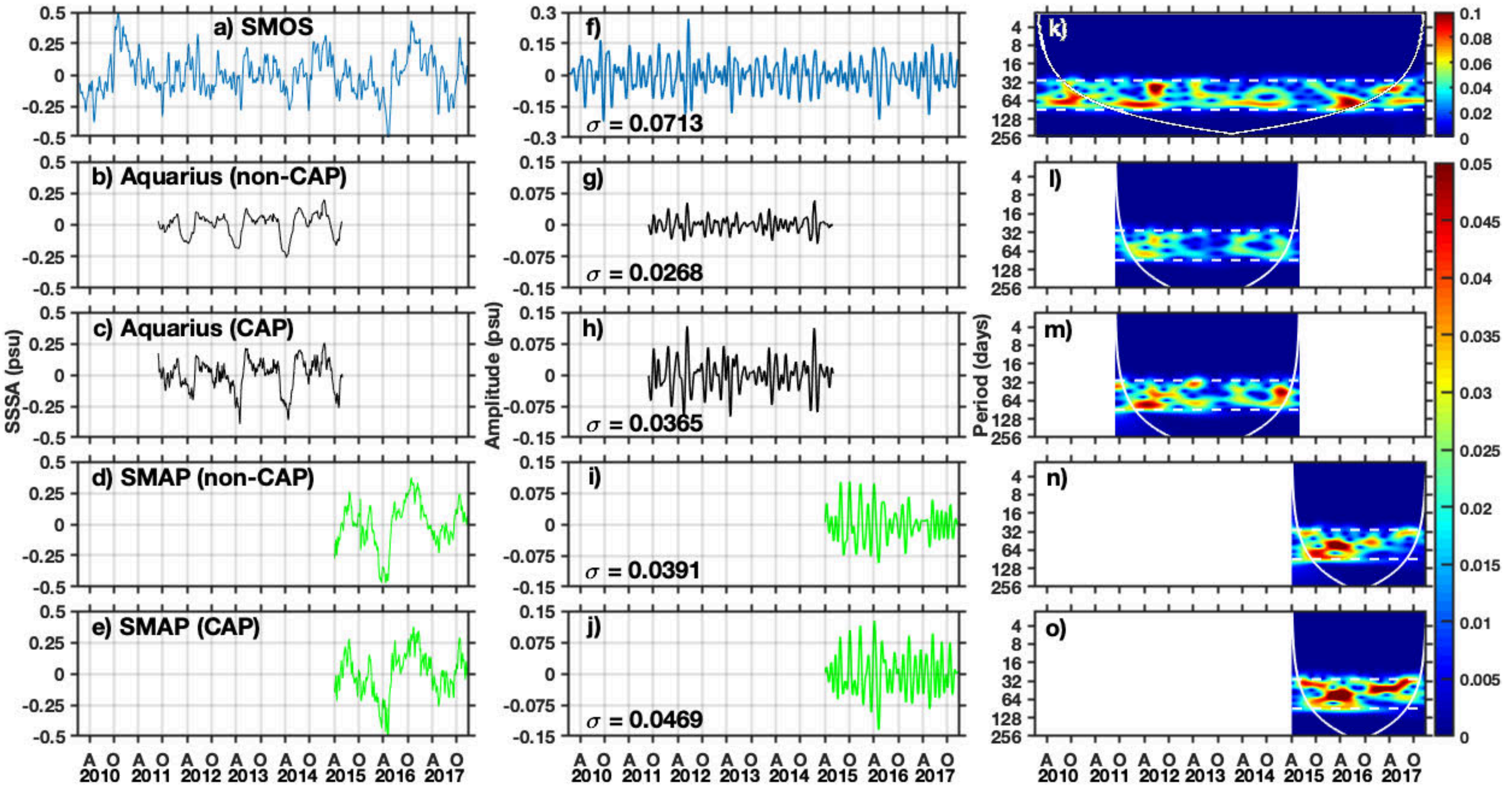

(a-e) 40°E-100°E, 5°S-5°N box averaged SSSA (psu); (f-j) 30-90-day filtered of a-e (psu); (k-o) Continuous wavelet transform of the SSS signals. White dashed lines represent the 30 and 90 day periods; White solid line denotes the cone of influence. April (A) and October (O) are indicated for each year.

Shoup et al., (2019)

30-90-DAY ISO

- Comparison of all 5 satellite SSS products from 2010-2017
- SMOS has the strongest MJO signal
- CAP processing gives Aquarius a comparable signal strength in eastern Indian Ocean to SMAP, SMOS
- CAP processing improves SMAP significantly, especially east of 60°E and near the Maritime Continent

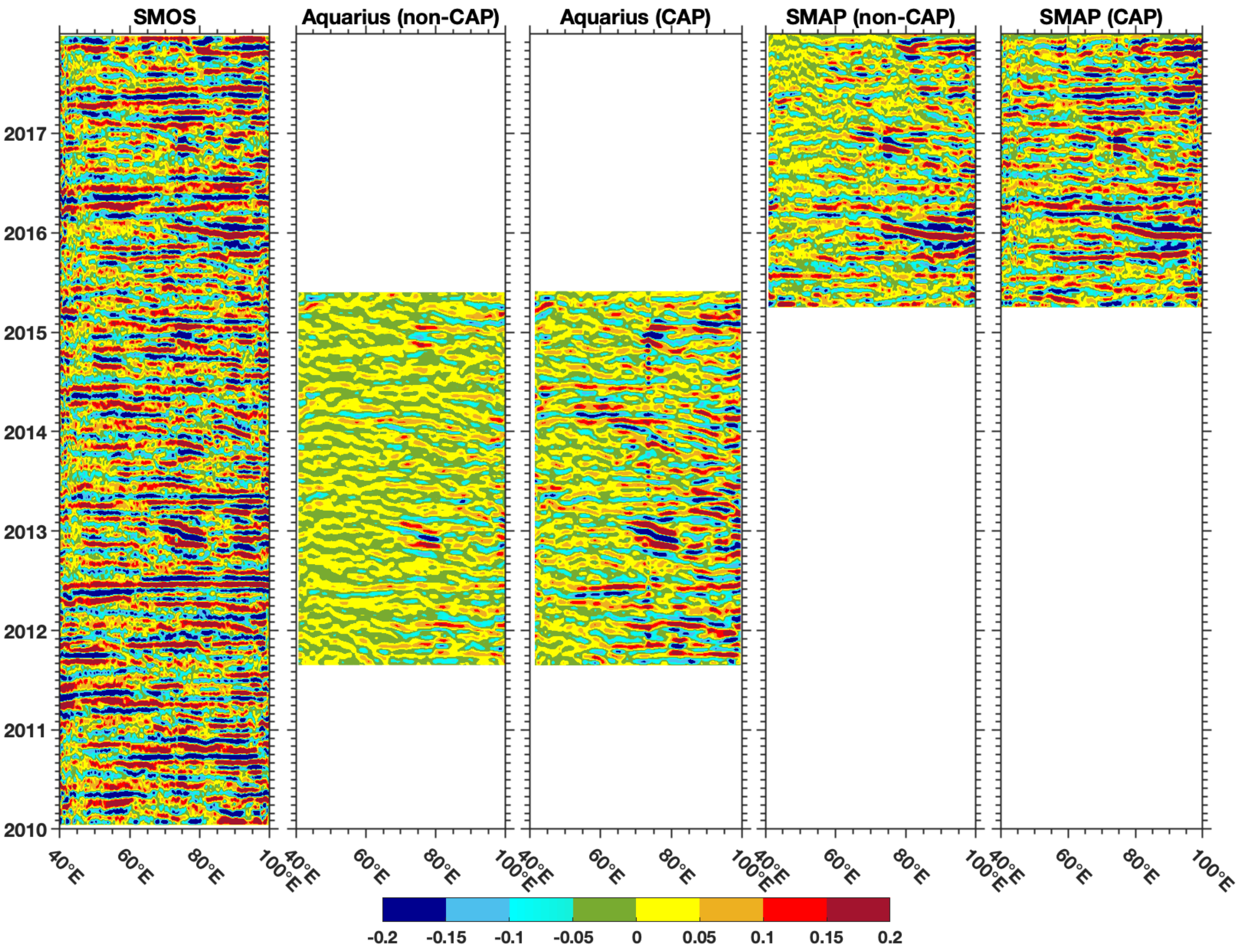

Time-longitude Hovmöller plot of 30-90-day bandpass filtered non-CAP and CAP SSS (psu) products latitudinally averaged over 5°S-5°N.

Shoup et al., (2019)

QUASI-BIWEEKLY OSCILLATIONS (10-20-DAY)

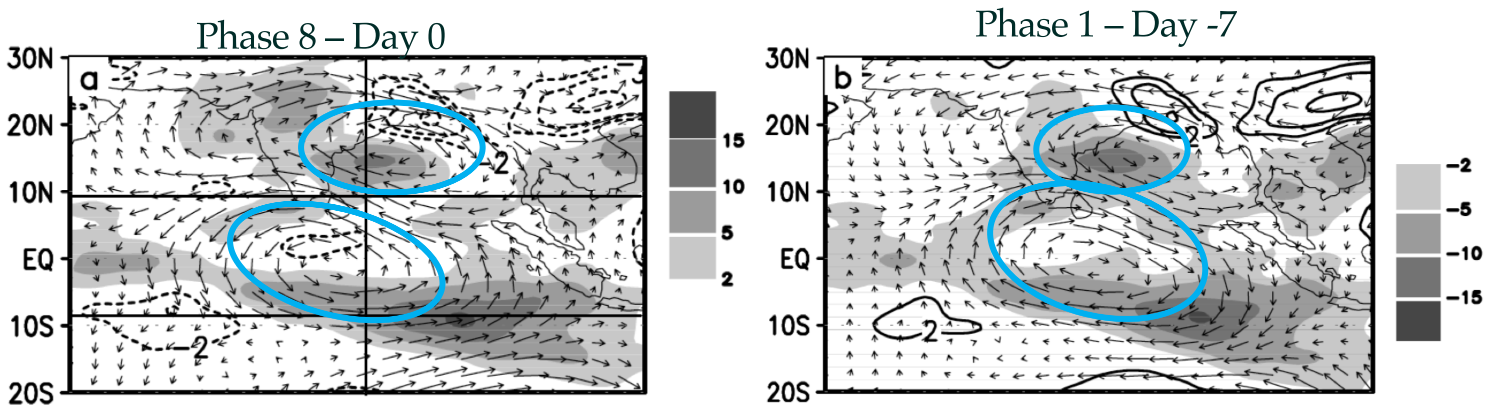

- **Overview:**
- One of the main controls on active/break cycles of monsoon rainfall
- Propagation speed: 4.5-6 ms^{-1} (NW or W)
- Dominant wavelength: 6,000 km

Double cell structure of the 10-20-day ISO during Phase 1 (Day -7) and Phase 8 (Day 0), where Day 0 is the day of maximum precipitation in the Bay of Bengal. Shading indicates TRMM precipitation, vectors are 850 mb winds, (Chatterjee and Goswami, 2004)

- **Structure and dynamics:**
- Double-cell structure of either lows or highs around the equator and 15-20°N
- Structure propagates west, where the northernmost cell propagates along the monsoon trough → Mixed Rossby Gravity Waves translated north in the atmosphere
- Triggered by breaking Rossby Waves in upper atmosphere over Northern Pacific Ocean into the South China Sea/Western Pacific Ocean

MODEL SIMULATIONS AND REANALYSES

Nucleus for European Modeling of the Ocean version 3.4 (NEMOv3.4)

- 1/12° Global horizontal resolution and 50 vertically stratified depths → eddy resolving
- NEMO's latest version has 10-day forecasts from 2016 to present available in daily temporal resolution.
- This version assimilates altimeter data, *in situ* temperature and salinity vertical profiles, and satellite-derived SST.
- Also using the reanalysis version, ORAS5

NOAA/NCEP Climate Forecast System version 2.0 (CFSv2.0)

- Atmosphere-land-ocean-ice coupled model
- Resolution of 0.25° at 6-hr intervals from 2011-present (CFSR is from 1979-2011) with 40 vertical layers

Estimating the Circulations and Climate of the Ocean (ECCO)

- Ocean state estimate from JPL
- Resolution of 1° with 50 vertical layers
- Available from 1992-2017 daily and monthly

10-20-DAY ISO

- Upper left: GPM Precipitation anomalies
- Upper right NEMO MLD anomalies
- Bottom left: NEMO SST anomalies
- Bottom right: NEMO SSS anomalies

- Mixed layer deepens with increased precipitation
- SSTs cool following high precipitation
- Weak SSS signal

Day -7

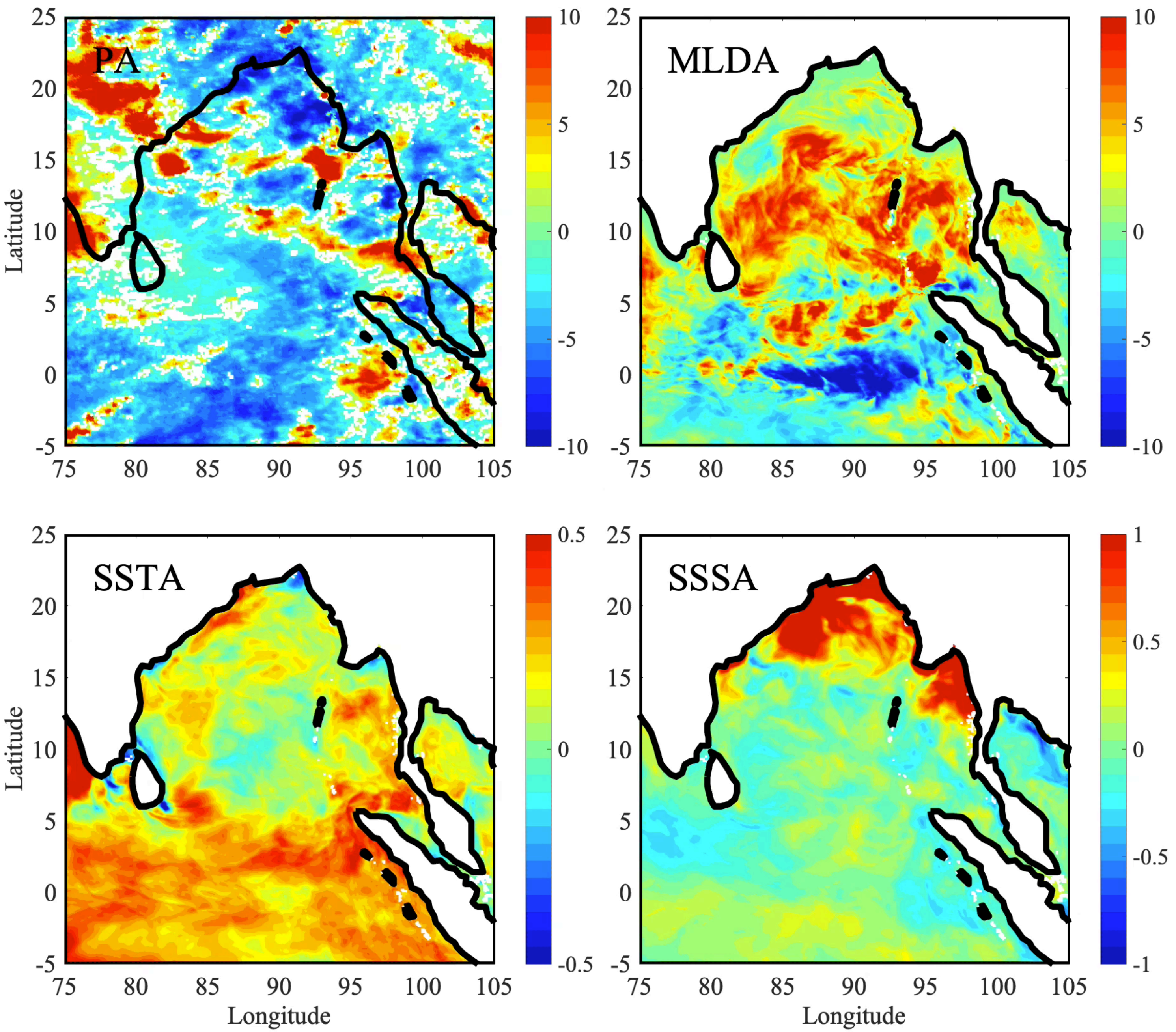

10-20-DAY ISO

- 10-20-day bandpass filtered NEMO temperature and salinity with depth for May-October 2016
- Temperature signal strongest in Southern, Equatorial BoB below MLD to 250 m
- Salinity signal weaker than temperature, strongest at surface in Northern BoB above MLD, penetrates down to ~100 m

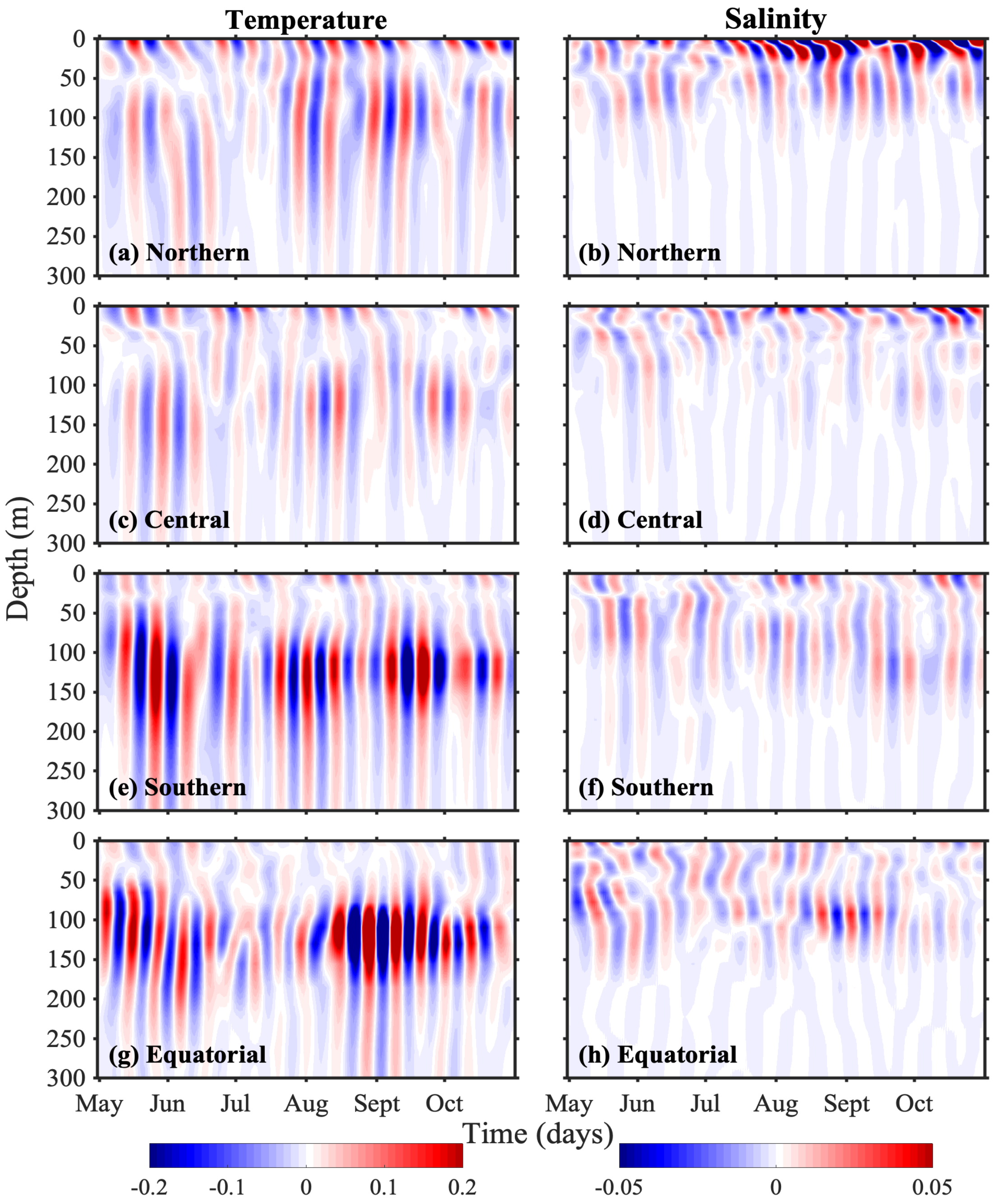

10-20-day bandpass filtered depth-time diagrams for NEMO temperature (left; °C) and salinity (right; shaded; psu) anomalies, box-averaged in the (a-b) Northern (85-100°E, 15-20°N), (c-d), Central (85-100°E, 10-15°N), (e-f) Southern (85-100°E, 5-10°N), and (g-h) Equatorial (85-100°E, 0-5°N) Bay of Bengal for May-October 2016.

Roman-Stork et al., (2019)

SYNOPTIC SCALE OSCILLATIONS (3-7-DAY)

- Associated with weather systems (highs and lows)
  - Tropical convergence zone (TCZ) over continent in active spells, over equatorial Indian Ocean in break spells
- TCZ = ascending branch of local Hadley circulation
  - During NH summer located around 25°N over India
- Wavelength of 2000 km
- TCZ and 3-7-day mode both modulated by other ISOs and interannual variability
  - Spatial/temporal structure of TCZ consistent with 30-60-day mode
  - Variations in monsoon trough → variations in monsoon rainfall

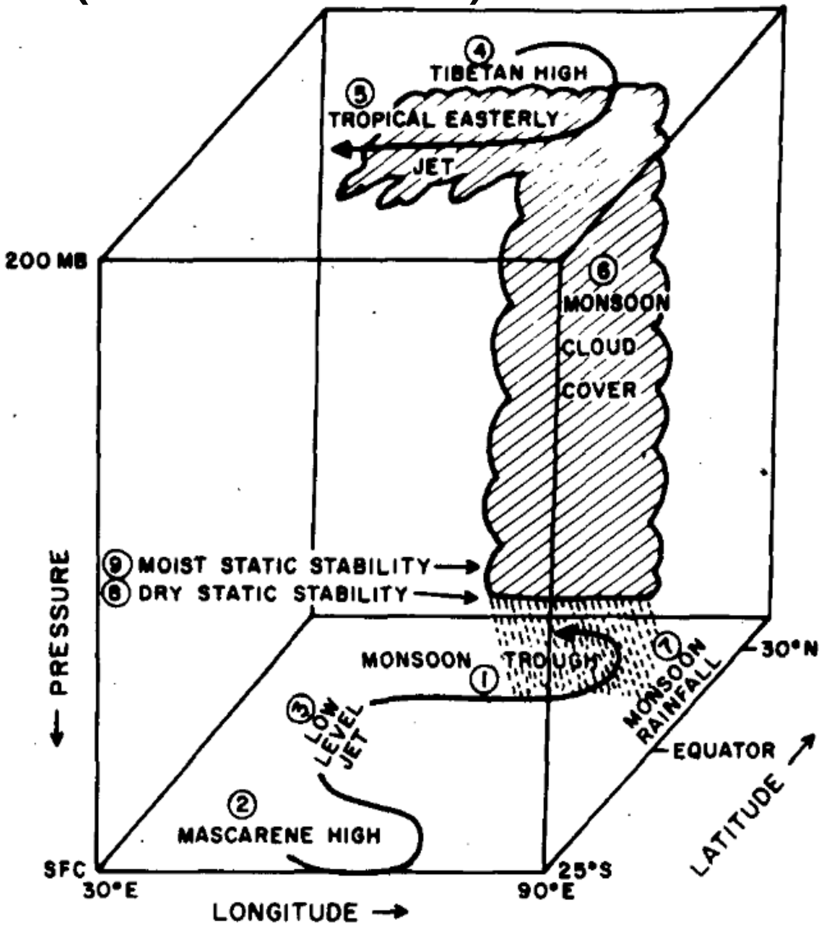

FIG. 1. Schematic diagram of the nine elements of the monsoon system considered in this study.

Krishnamurti and Bhalme (1976)

3-7-DAY ISO

- GPM precipitation over central India with active and break phases
- 3-7-day mode explains 48% of observed rainfall variability in central India
- 3-7-day mode modulated by other ISOs

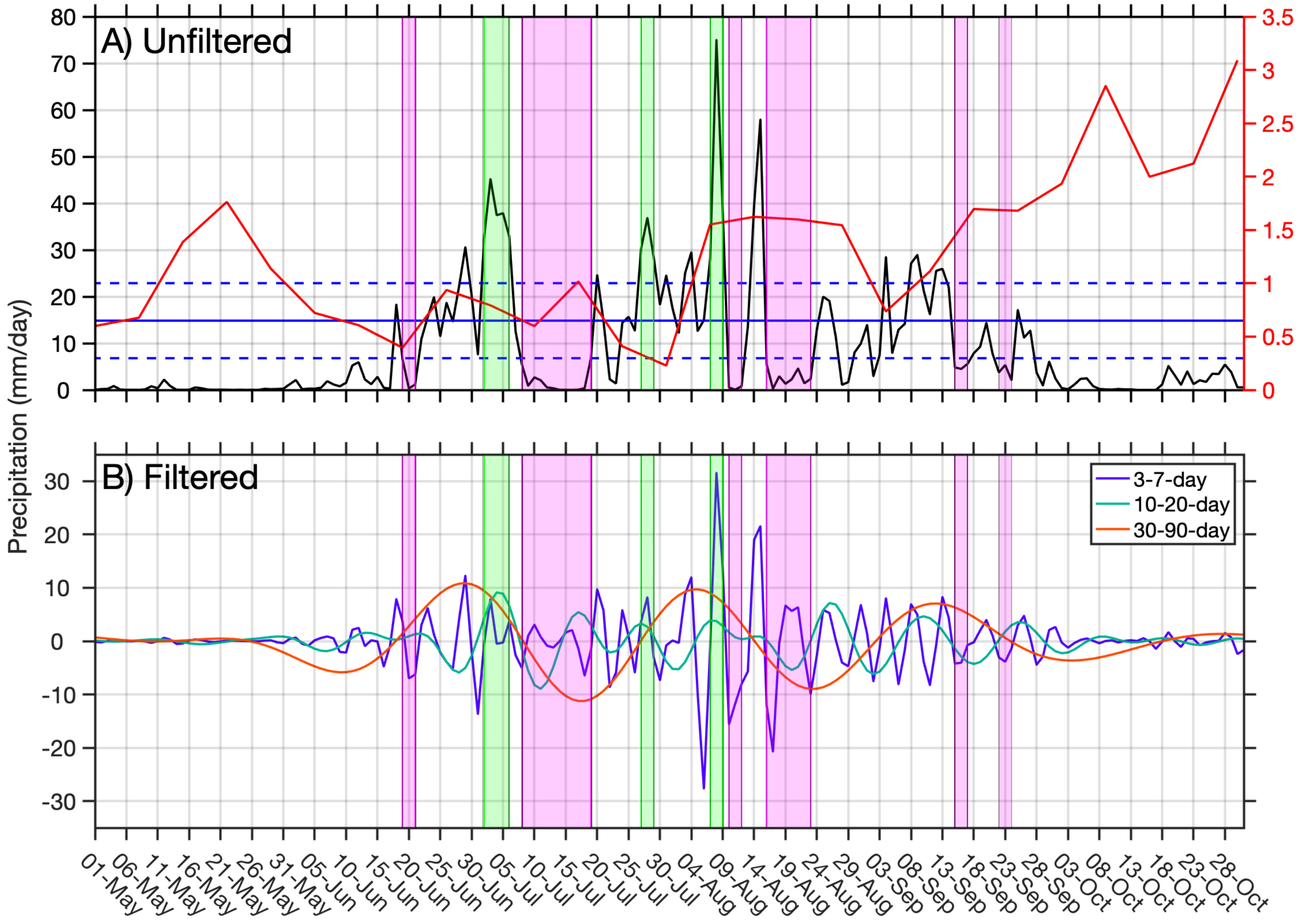

Subrahmanyam et al., (2020)

Box averaged time series of (top) unfiltered GPM precipitation over the central India (73-78E, 20-25N) (black; mm/day) and Dipole Mode Index (DMI; red; °C) and (bottom) bandpass filtered with 3-7-day synoptic oscillations (purple; mm/day) and 10-20-day ISO (teal; mm/day) and 30-90-day ISO (orange; mm/day) GPM precipitation in the same northern India box. In the top figure, solid blue line indicates the mean July/August rainfall over central India, blue dashed lines indicate ±0.5 standard deviation. Weekly DMI values are retrieved from NOAA and are calculated from OISST data as DMI West (50-70E, 10S-10N) minus DMI East (90E-110E,10S-0N). In the bottom figure, active phases of the monsoon are indicated by green boxes; magenta boxes indicate break phases based on criteria from Singh and Nakamura (2010).

3-7-DAY ISO

- 3-7-day filtered satellite observations for the 2019 monsoon season (May-October) by region in the Bay of Bengal
- 3-7-day signal detectable in all parameters
- Strongest signals in late season (August-October)
- Spikes in precipitation consistent with SSS in northern, southern Bay

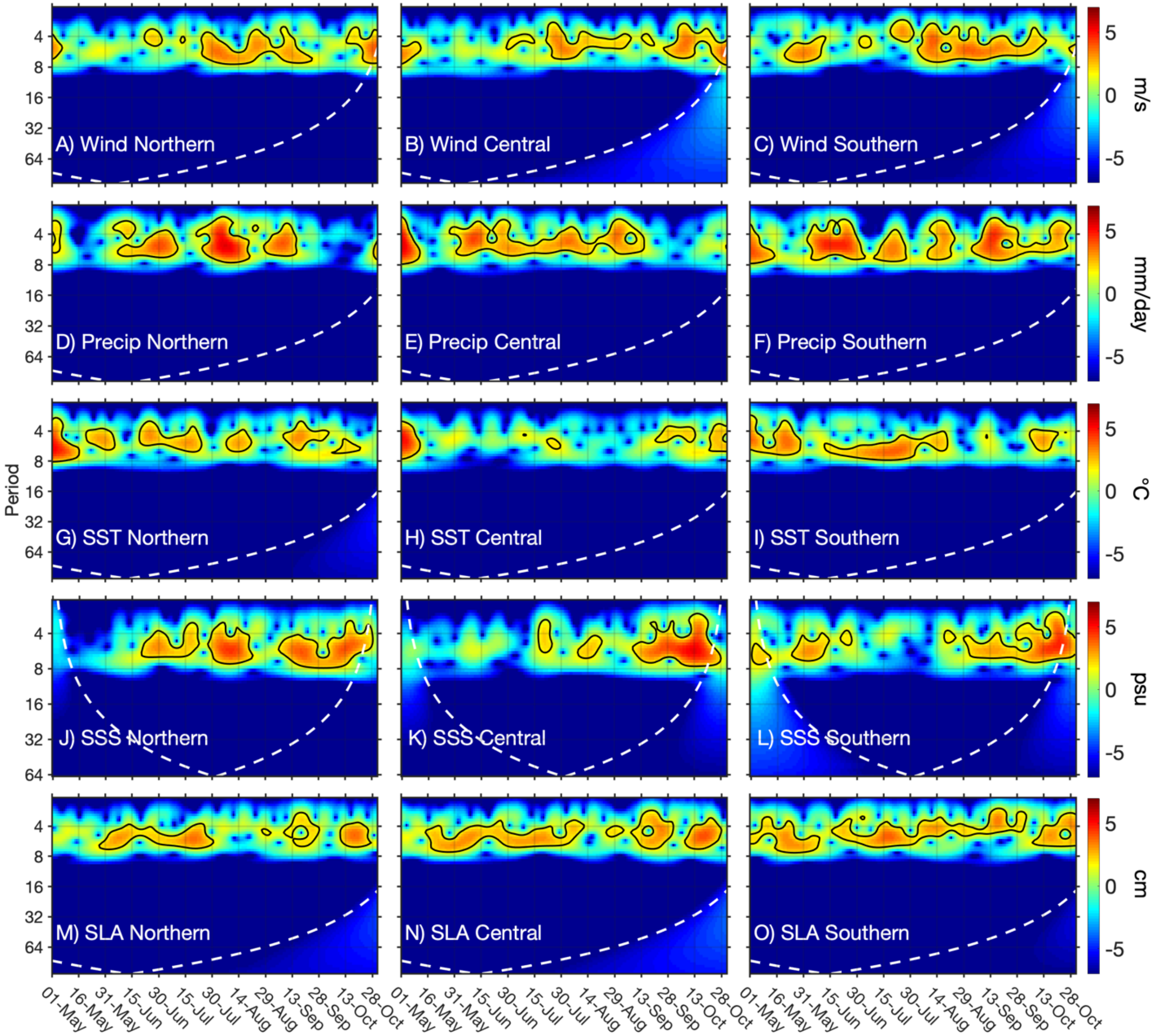

Subrahmanyam et al., (2020)

Wavelet analysis of surface wind speed (A-C; m/s), GPM precipitation (D-F; mm/day), OISST (G-I; ℃), NEMO SSS (J-L; psu), and CMEMS SLA from blended altimetry (M-O; cm) bandpass filtered with the 3-7-day period synoptic oscillations over the boxes in the northern (A,D,J,M; 15-20N), central (B,E,H,K,N; 10-15N), and southern (C,F,I,L,O; 5-10N) Bay of Bengal.

3-7-DAY ISO

- 3-7-day filtered **NEMO** for the 2019 monsoon season (May-October) by region in the Bay of Bengal
- 3-7-day salinity signal in mixed layer and along thermocline, especially in southern/equatorial
- Temperature signal only below thermocline and only strong in southern/equatorial Bay → eddy processes

Subrahmanyam et al., (2020)

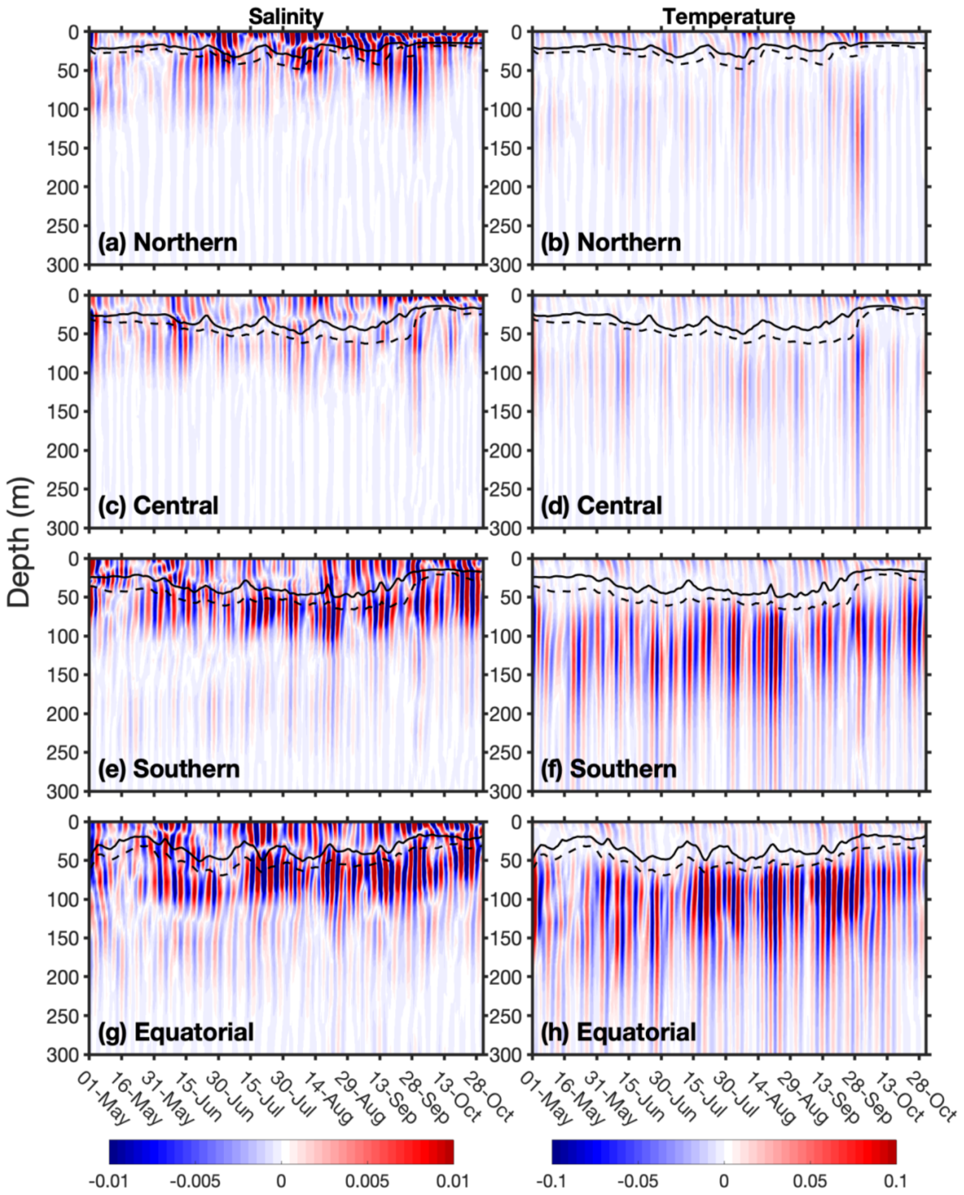

Depth-time cross-sections of 3-7-day bandpass filtered NEMO salinity (left; psu) and temperature (right; °C) anomalies, box-averaged in the (a-b) Northern (85-100°E, 15-20°N), (c-d), Central (85-100°E, 10-15°N), (e-f) Southern (85-100°E, 5-10°N), and (g-h) Equatorial (85-100°E, 0-5°N) Bay of Bengal for May-October 2019. Calculated isothermal layer depth (ILD; m; black dashed line) and mixed layer depth (MLD; m; black solid line) are overlaid.

Eddy Variability and Connections to Atmospheric Convection in the Bay of Bengal

COASTAL KELVIN WAVES

- 4 coastal Kelvin waves in the Bay of Bengal
  - 2nd downwelling arrives in Oct-Nov
  - Radiates Rossby Waves that trigger eddying in the EICC region
- All caused by equatorial wind stress perturbations
  - Strength and timing influenced by speed, duration, and width of perturbation
- Off equatorial RWs feedback into equatorial KWs, strengthen coastal KWs in the Bay

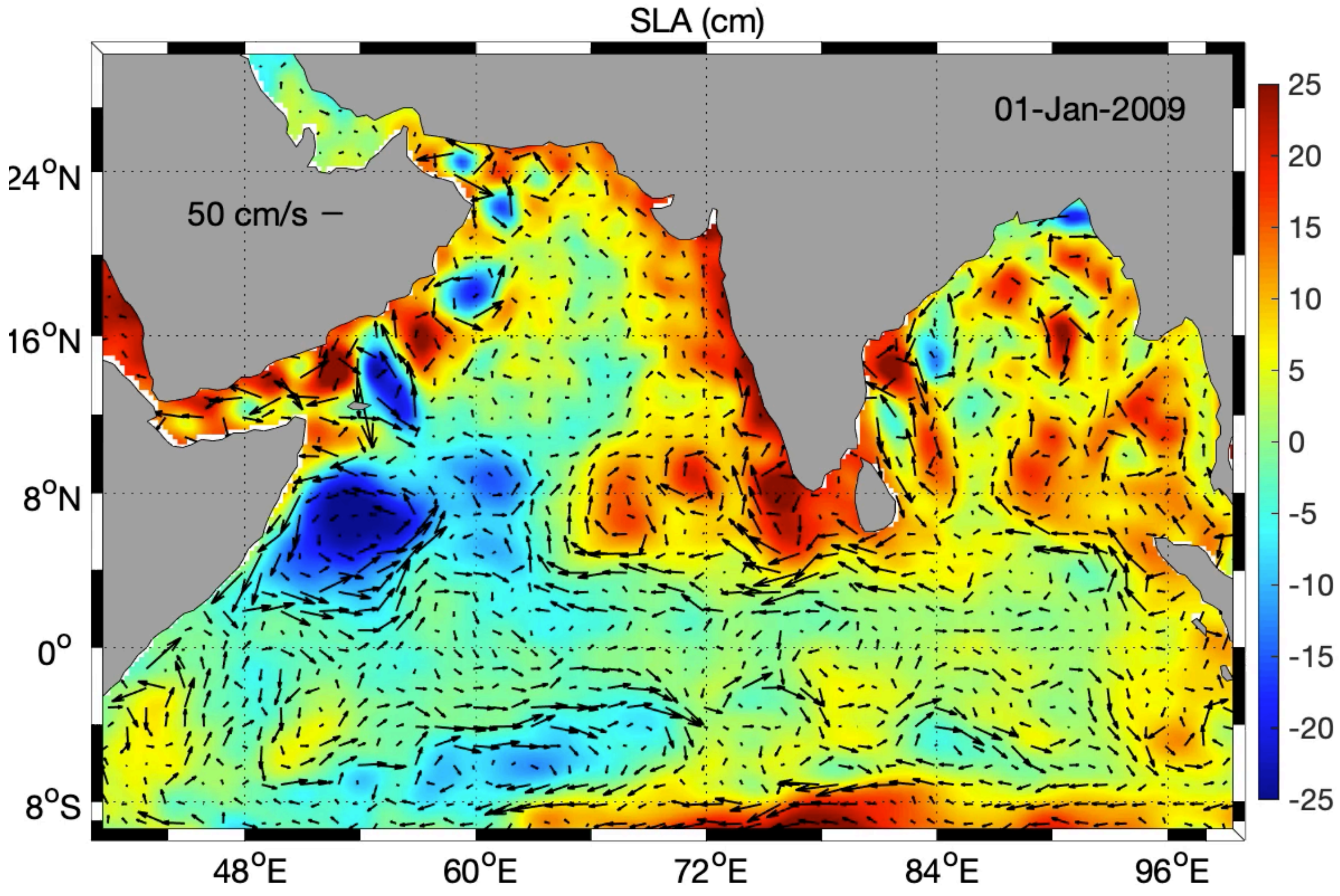

CMEMS blended altimetry sea level anomalies (SLA; cm) overlaid with geostrophic currents (cm/s) in the Northern Indian Ocean from 2009 through 2018

EDDY TRACKING

- Using a closed contour eddy tracking methodology, found all mesoscale eddies in the BoB from 1993-2018
- Large numbers of anticyclonic eddies (AEs) in the northern and eastern BoB
- Most cyclonic eddies (CE) in the northwestern and eastern BoB
- Largest eddies, EKE in the western BoB along EICC
- Most eddies generated along eastern coasts

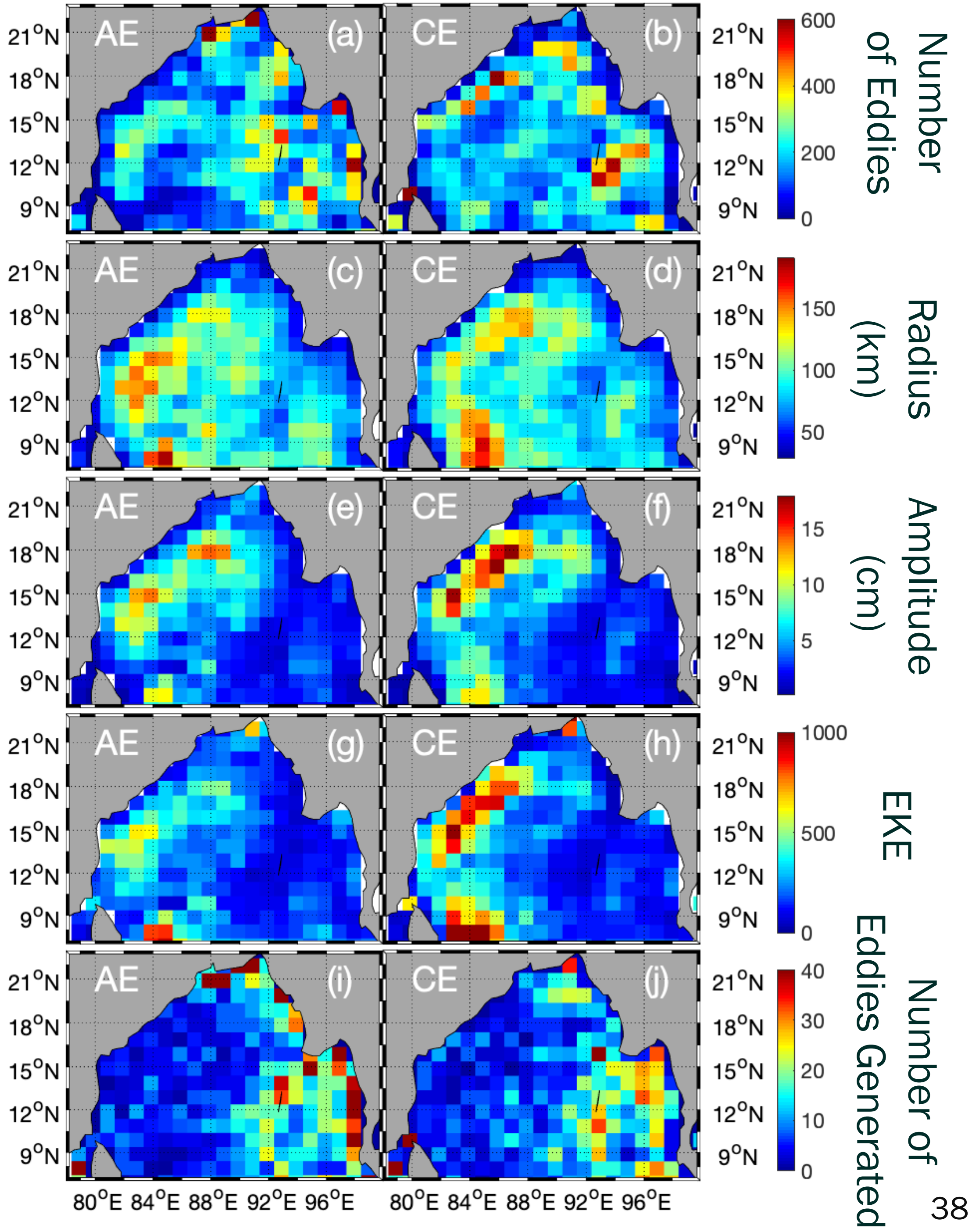

Mean spatial distribution of eddy characteristics for the Southwest monsoon season (Jun-Sep) from 1993-2018 for AEs (left panel) and CEs (right panel). (a-b) Number of eddies; (c-d) radius (in km); (e-f) amplitude (in cm); (g-h) EKE (in cm^2 s^{-2}); (i-j) Number of eddy generation.

Roman-Stork et al., (2019)

SURFACE AND SUBSURFACE EDDY STRUCTURE

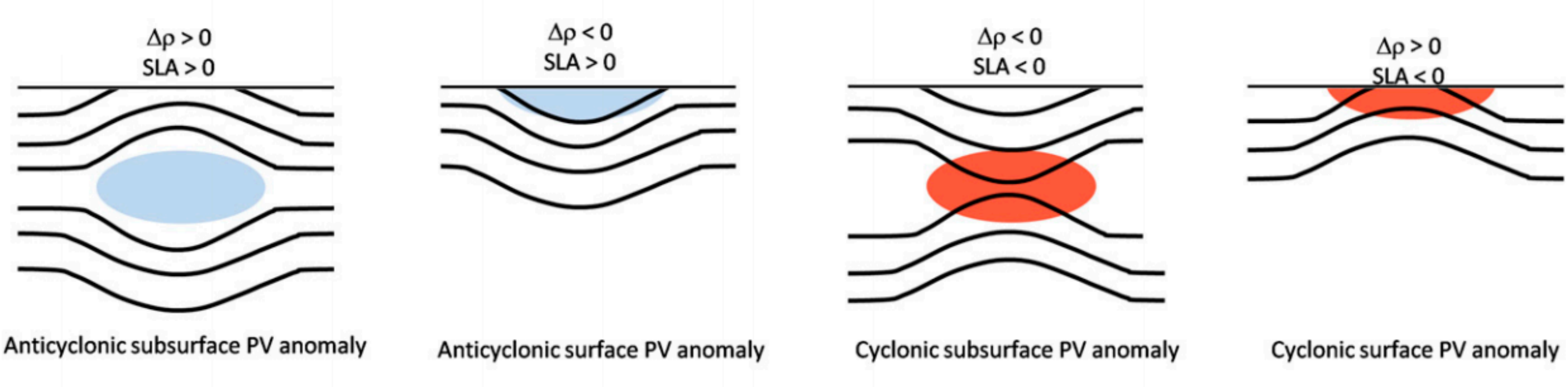

- Surface-intensified eddies have the maximum of PV at the surface, doming of isopycnals below maximum of PV
- Subsurface-intensified eddies have maximum of PV below the surface with doming of isopycnals above and below maximum of PV

(Assassai et al., 2016)

EDDIES, SST, AND CONVECTION

- Composites of anticyclonic (top) and cyclonic eddies (bottom) that are surface/subsurface intensified and warm/cold core
- For all eddy SLA and SSTA types, OLR is locally low (high) when SSTA is locally high (low)
- Strongly suggests connection between warm eddies and convection over the BoB

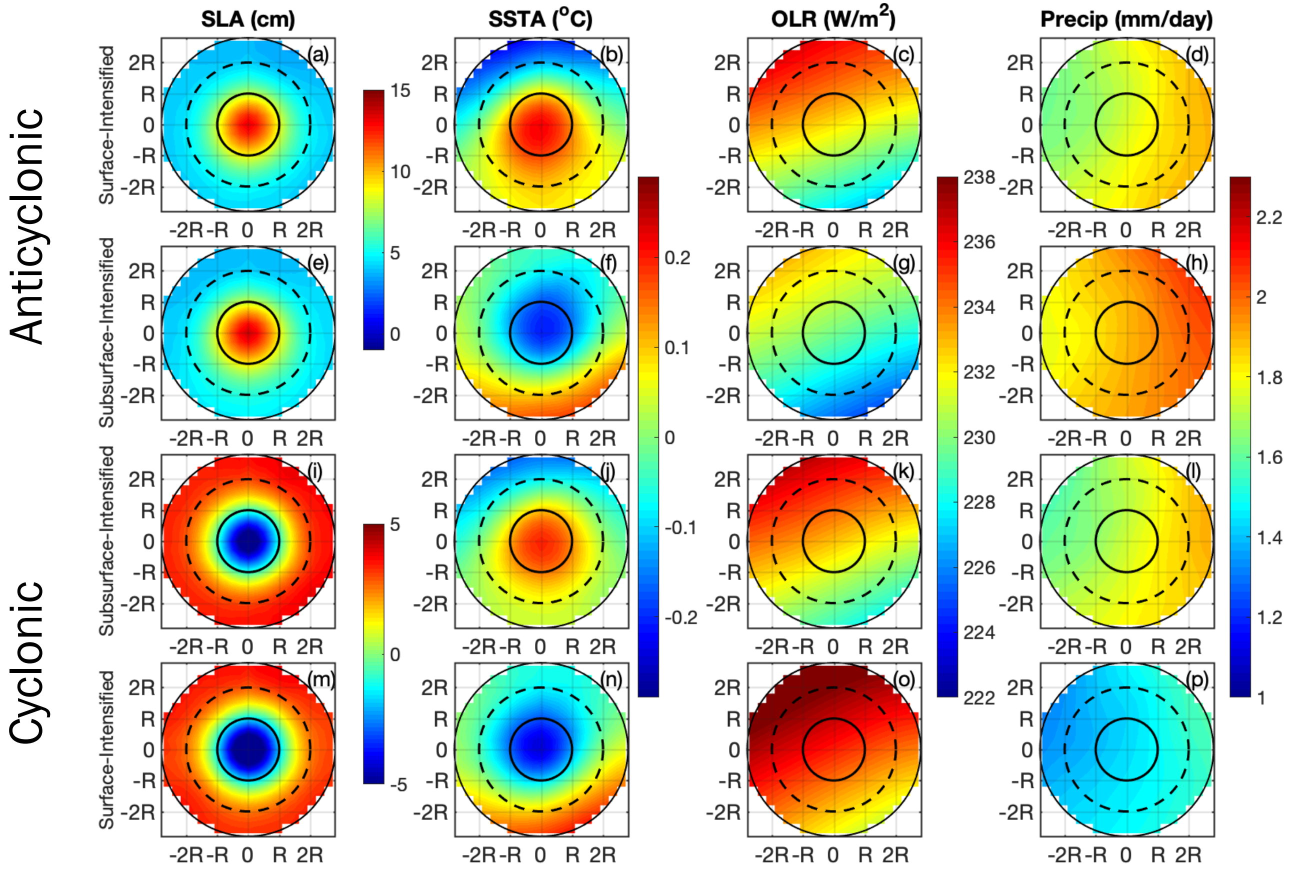

Eddy composites with normalized radius for 1993-2018 in the Bay of Bengal in SLA (left; cm), SSTA (left middle; ℃), OLR (right middle; W/m^2), and precipitation (right; mm/day) for (a-d) surface intensified warm core AEs, (e-h) subsurface-intensified cold core AEs, (i-l) subsurface intensified warm core CEs, and (m-p) surface intensified cold core CEs.

Roman-Stork et al., (2019)

CURRENT ALTIMETERS

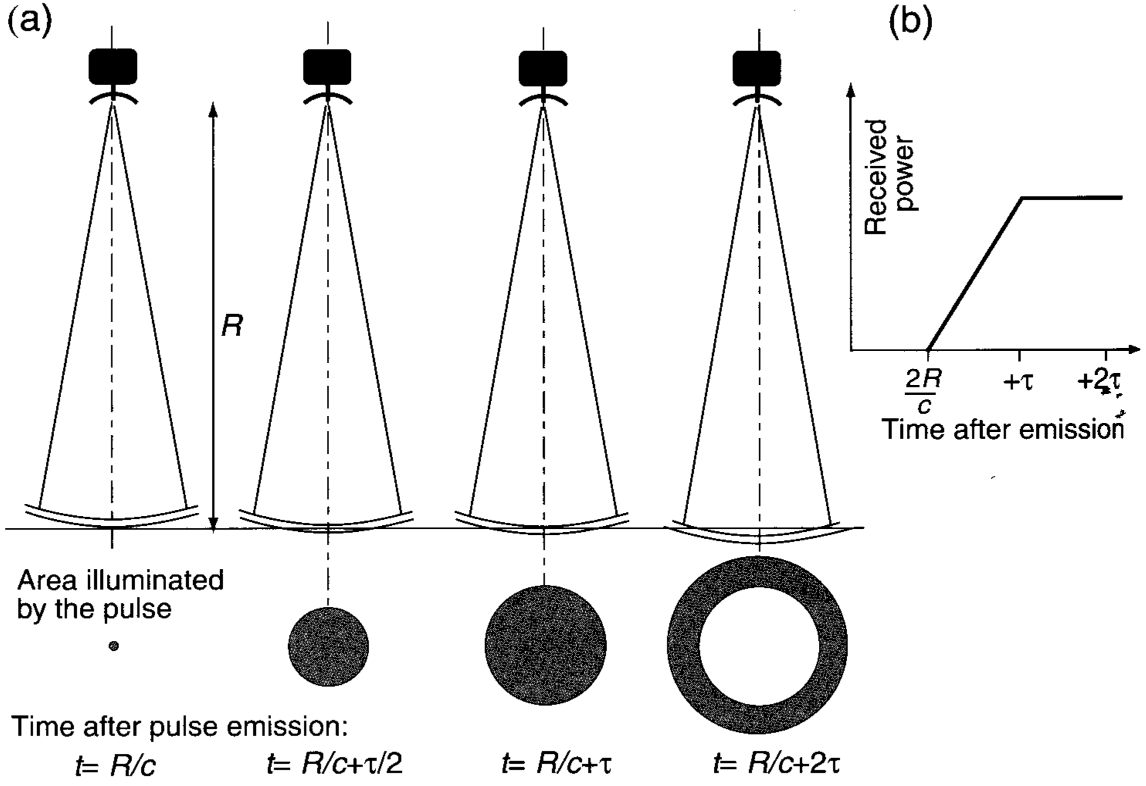

Interaction of the pulse of duration τ with a smooth sea surface.

For an altimeter in a 1000-km orbit a pulse duration of about 3 ns would lead to a footprint of diameter 2.8 km.

SWOT MISSION

- Surface Water and Ocean Topography (SWOT) Mission
- Joint NASA, CNES, UK, and Canada mission
- Set to launch in 2022
- Uses SAR imagery (120 km swath) in conjunction with radiometer at nadir to measure SSH
- Measures both SSH and surface water (rivers, lakes, etc.)
- 21-day repeat cycle
- Spatial resolution <9-15 km
- Will be able to measure submesoscale features

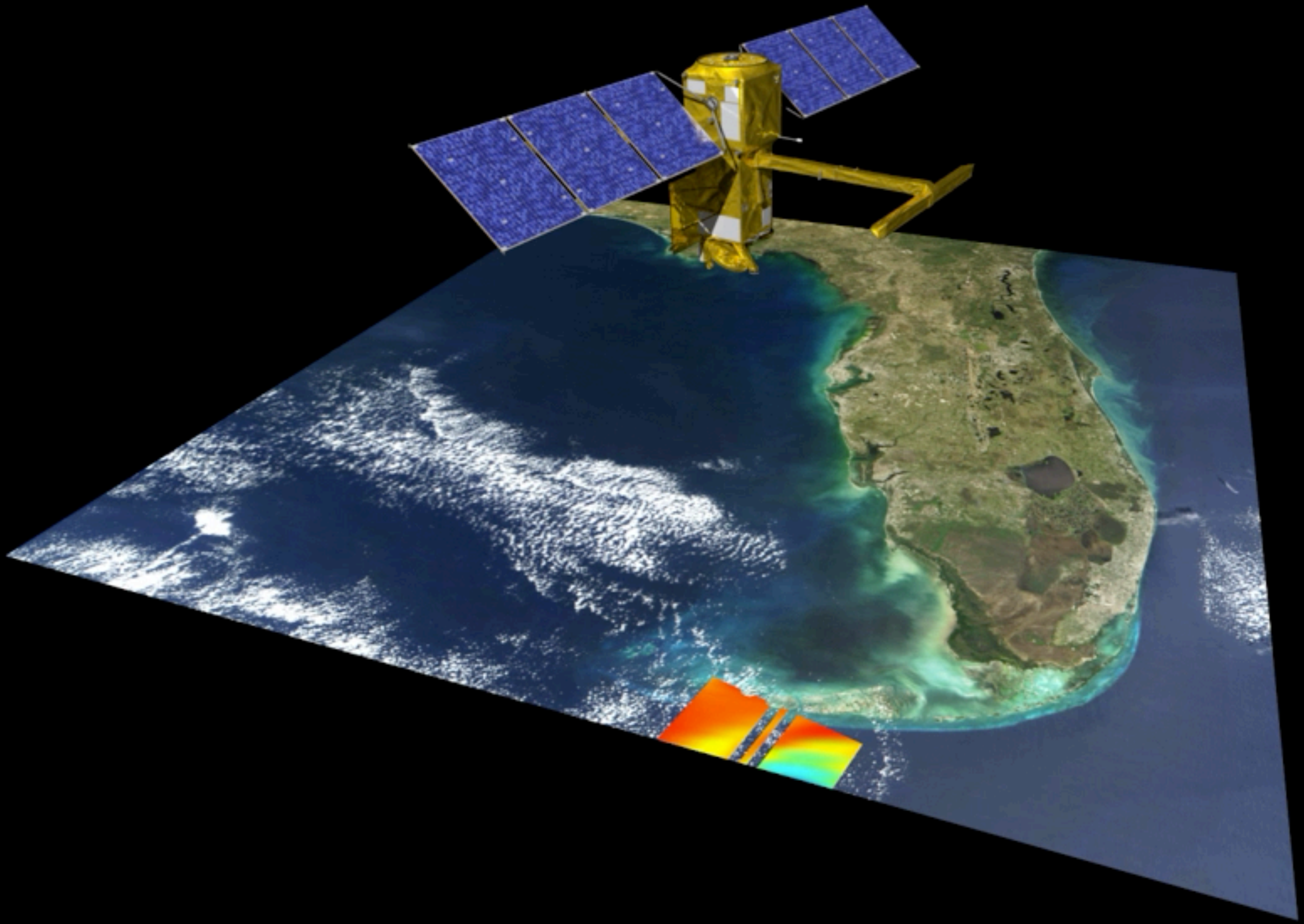

OCEAN COLOR

- Numerous ocean color products now exist, including blended daily products
- Can clearly see both mesoscale and submesoscale eddies
- Reflects changes in productivity associated with eddy variability

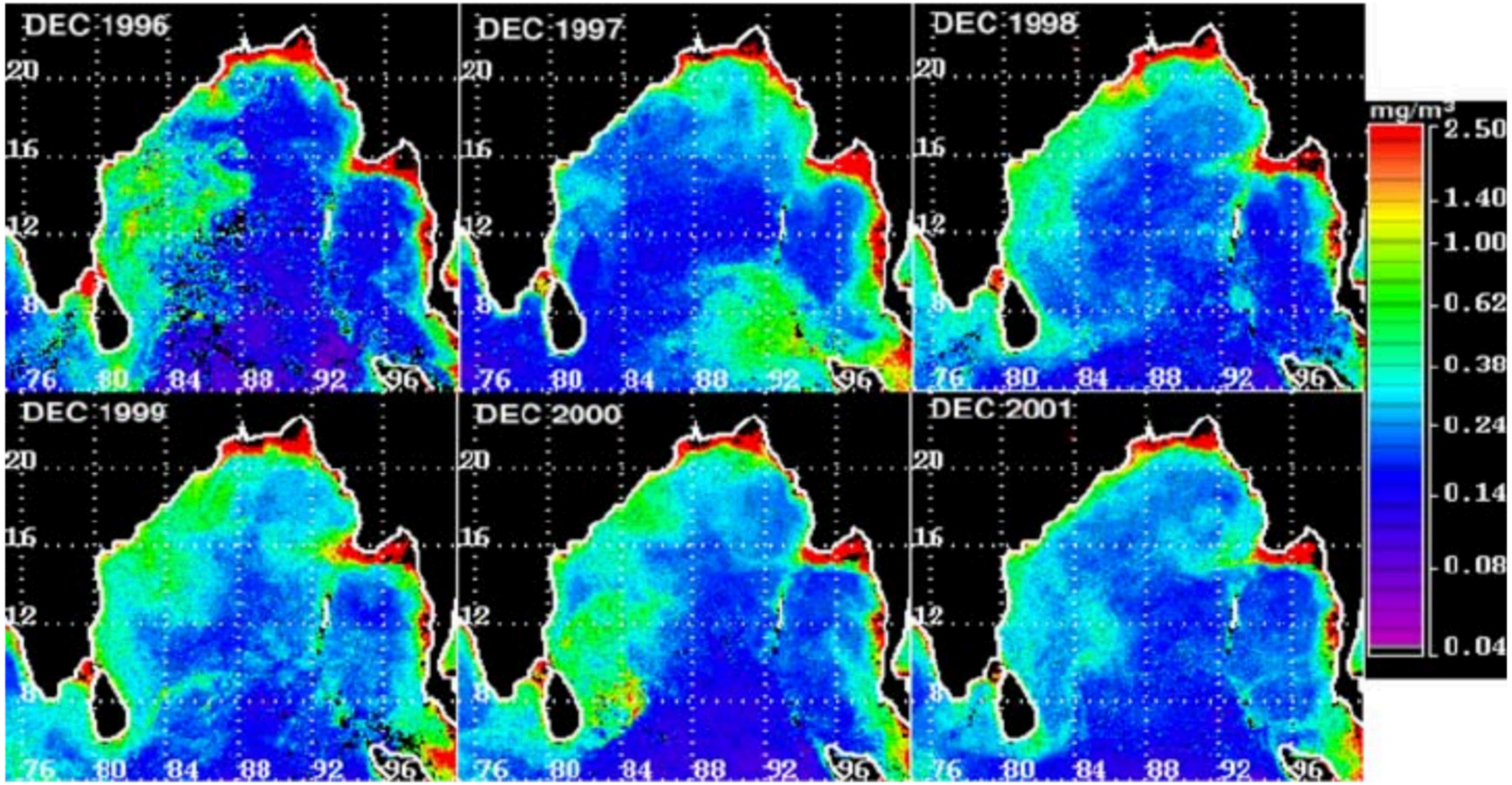

December composites of chl-a (mg/m^3) derived from OCTS for 1996 and from SeaWiFS for 1997-2001. From Vinayachandran and Mathew (2003).

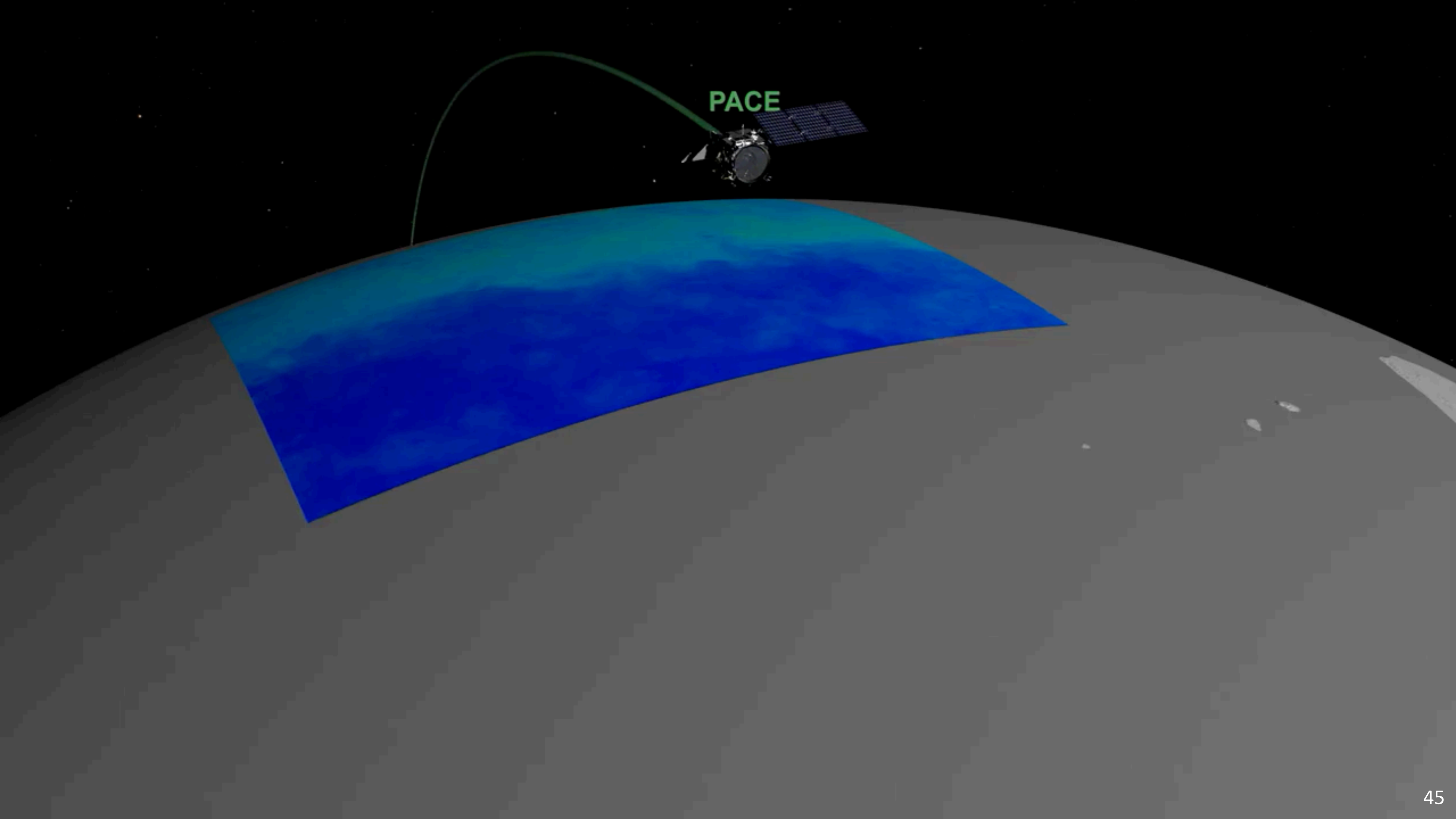
PACE

Summary

- Salinity, barrier layer thickness (BLT), and moisture flux control monsoon onset and strength in the SEAS
- Satellite-derived salinity from SMAP can and should be used to monitor and forecast the southwest monsoon through freshwater fluxes and barrier layer development
- SMAP salinity and satellite altimetry can be used to monitor all ISOs in the Bay of Bengal, including 3-7-day synoptic oscillations
- The addition of SWOT altimetry will allow for tracking of submesoscale eddies in the Bay of Bengal and more accurate monsoon forecasting
- PACE and SWOT will allow for multiparameter mesoscale and submesoscale eddy tracking

Future Work

- Identification of internal waves and characteristics in the Bay of Bengal using SAR imagery
- Observing ocean freshwater flux using satellite observations (SSS and currents)
- Analyzing Indian Ocean fronts using satellite-derived SSS, SST, SLA, and ocean color
- Exploring the impact of salinity on Indian Ocean mixed layer variability
- Determining the role of the Agulhas current in the global ocean circulation, climate, and ecosystem dynamics
- Tracking of mesoscale and submesoscale structures in the Indian Ocean using satellite-derived SSS, SST, SLA, and ocean color (using SWOT and PACE)

Broader Impacts

- The assimilation of satellite SSS in model simulations will improve forecasting of monsoon timing and intensity
- Utilization of SSS, SLA, and ocean color for monitoring of monsoon processes
- Salinity and temperature variations impact the spatial density field and the mixed layer during ISO propagation
  - The dynamics associated with the mixed layer formation are important for acoustic propagation and its predictions.
- Over 1 billion people are directly impacted by monsoon rainfall
  - Impacts on agriculture, economics (local and global), shipping routes, fisheries, personal wellbeing, and national security

Acknowledgments

PhD Committee

Prof. Subrahmanyam Bulusu (PhD Advisor)

Prof. Alexander Yankovsky

Prof. Jay Pinckney

Dr. Anthony Arguez (NOAA NCEI)

Satellite Oceanography Lab

Rachel, Ricky, Casey, Corinne, Brady, and Sam

PUBLICATIONS

- Shoup, C. G., **H.L. Roman-Stork,** and B. Subrahmanyam (2020). Analysis of Coupled Oceanic and Atmospheric Preconditioning for Primary Madden-Julian Oscillation Events, Journal of Geophysical Research: Oceans (*In review*)
- Subrahmanyam, B., **H.L. Roman-Stork,** and V.S.N. Murty (2020). Monitoring of Synoptic Signals and Low-Pressure Systems in the Indian Ocean during the 2019 Southwest Monsoon, Journal of Geophysical Research: Oceans 125, e2020JC016200, https://doi.org/10.1029/2020JC016200
- **Roman-Stork, H.L.,** B. Subrahmanyam, and C.B. Trott (2020). Monitoring Intraseasonal Oscillations in the Indian Ocean using Satellite Observations, Journal of Geophysical Research: Oceans, 125, e2019JC015891. https://doi.org/10.1029/2019JC015891
- **Roman-Stork, H.L.,** B. Subrahmanyam, and V.S.N. Murty (2019). The Role of Salinity in the Southeastern Arabian Sea in Determining Monsoon Onset and Strength. Journal of Geophysical Research: Oceans, 125, https://doi.org/10.1029/2019JC015592
- **Roman-Stork, H.L.,** B. Subrahmanyam, and C.B. Trott (2019). Mesoscale Eddy Variability and its Linkage to Deep Convection over the Bay of Bengal using Satellite Altimetric Observations, Advances in Space Research, https://doi.org/10.1016/j.asr.2019.09.054.
- **Roman-Stork, H.L.,** B. Subrahmanyam, and V. S. N. Murty (2019). Quasi-biweekly Oscillations in the Bay of Bengal in Observations and Model Simulations, Deep Sea Research II, https://doi.org/10.1016/j.dsr2.2019.06.017.
- Trott, C.B., B. Subrahmanyam, A. Chaigneau, and **H.L. Roman-Stork** (2019). Eddy-induced Temperature and Salinity Variability in the Arabian Sea, Geophysical Research Letters, 46. https://doi.org/10.1029/2018GL081605
- Trott, C.B., B. Subrahmanyam, **H.L. Roman-Stork**, V.S.N Murty, and C. Gnanaseelan (2019). Variability of Intraseasonal Oscillations and Synoptic Signals in Sea Surface Salinity in the Bay of Bengal, Journal of Climate. https://doi.org/10.1175/JCLI-D-19-0178.1
- Shoup, C. G., B. Subrahmanyam, and **H.L. Roman-Stork** (2019). Madden-Julian Oscillation-Induced Sea Surface Salinity Variability as Detected in Satellite-Derived Salinity. Geophysical Research Letters. https://doi.org/10.1029/2019GL083694